ENERGY AND BUILDINGS

Quantifying Demand Balancing in Bidirectional Low Temperature Networks

Marco Wirtz, Lukas Kivilip, Peter Remmen, Dirk Müller

RWTH Aachen University, *E.ON Energy Research Center, Institute for Energy Efficient Buildings and Indoor Climate, Mathieustr. 10, Aachen, Germany*

Please cite journal article:
https://www.sciencedirect.com/science/article/pii/S0378778820309889

DOI: 10.1016/j.enbuild.2020.110245

Accepted manuscript

Quantifying Demand Balancing in Bidirectional Low Temperature Networks

Marco Wirtz[a,*], Lukas Kivilip[a], Peter Remmen[a], Dirk Müller[a]

[a] *RWTH Aachen University, E.ON Energy Research Center, Institute for Energy Efficient Buildings and Indoor Climate, Mathieustr. 10, Aachen, Germany*

Abstract

Bidirectional low temperature networks (BLTNs) are a promising technology to drive decarbonization of the heating and cooling sector. The energy efficiency of a BLTN strongly depends on the heating and cooling demands of the connected buildings and their simultaneity. In order to evaluate the efficiency of a BLTN, a novel metric, called *Demand Overlap Coefficient* (DOC), is presented in this paper. The DOC can be calculated for individual buildings or a district and describes which proportion of heating and cooling demands can be balanced *inside* buildings and *between* buildings. The DOC is calculated with time series for heating and cooling demands, taking special account of their simultaneity. For a real-world use case in Germany, it is shown that 25 % of heating and cooling demands can be balanced in buildings and 45 % can be balanced by the BLTN between buildings. The DOC is evaluated for 63 demand scenarios. Correlations show that for districts with a DOC larger than 0.45, BLTNs have lower annualized costs than a state-of-the-art heating and cooling system. BLTNs have higher exergy efficiencies for districts with

*Corresponding author

Email address: `marco.wirtz@eonerc.rwth-aachen.de` (Marco Wirtz)

DOCs larger than 0.3. With the derived correlations, the DOC serves as a practical key metric in the planning process of BLTNs in order to identify and assemble building clusters with complementary demand profiles.
Keywords:
Bidirectional low temperature network, 5GDHC, Waste heat, District heating, District cooling, Demand balancing

1. Introduction

Waste heat recovery is one key approach to increase the efficiency of energy systems, and thus to reduce fossil fuel consumption and carbon emissions [1]. The higher the temperature level of waste heat, the larger the economic and energy saving potential. For industrial processes with high process temperatures, waste heat recovery is a key approach to reduce costs and increase process efficiencies [2]: Recovered heat can be used in the process itself to increase its efficiency [3] or reused by other industrial or commercial processes [5], e.g. organic rankine cycle for electricity generation.

In the heating and cooling sector of commercial and residential buildings, waste heat, e.g. from cooling applications, usually remains unused due to its low temperature level. For example in data centers, low-grade waste heat is often dissipated ([6], [7]) instead of reusing it for other purposes, like district heating ([8], [9]).

Nevertheless, the energy saving potential of recovering low-grade waste heat is enormous since in urban districts the amount of waste heat can reach 50 – 120 % of the annual heat demand [10]. In addition, the importance of using low-grade waste heat sources will increase in future, since space cooling demands, as one major waste heat source, is expected to rise substantially in the coming decades [11]. Nowadays, space cooling is often provided by individual air conditioning units which dissipate waste heat to the environment.

To unlock urban waste heat potentials, a thermal connection between buildings through a central distribution infrastructure is crucial ([12], [13]) and recently gains more interest ([14], [15]). In the field of low temperature distribution grids, one promising concept are bidirectional low temperature networks (BLTNs) ([16], [17]), which are also referred to as *5th Generation District Heating and Cooling* (5GDHC) networks ([18], [19], [20], [21]), *cold district heating* ([22]), *low-temperature district heating and cooling networks* ([23], [24]) or *balanced energy networks* [25]. These networks are the latest development stage of district heating and follow the trend towards lower operating temperatures, as illustrated in Fig. 1.

BLTNs do not have a supply and return pipe, but a warm and cold pipe with a temperature difference of about 5 – 10 K. Both pipes are operated at temperatures close to the surrounding (5 – 35 °C). Due to the low temperatures, heating demands of buildings cannot be covered directly, and a heat pump is installed in each building to raise the temperature to the level required by the building's heating system. In heating mode, a heat pump takes water from the warm pipe and uses it as heat source. The cooled down water from the evaporator of the heat pump is then discharged to the cold pipe. If the building has a cooling demand, the fluid flow is opposite: Water from the cold pipe is warmed up in the building and discharged to the warm pipe. A detailed description is provided in [18] and [20]. One key advantage of BLTNs is that waste heat from a building with cooling demand can be reused to cover heating demands of other buildings. Thus, heating and cooling demands of a district are balanced out to some extent. Blacha et al. [26] and Rogers et al. [27] show that the amount of recovered heat, i.e. the share of balanced demands, has a strong impact on the performance of BLTNs. Boesten et al. suggest to consider demand profiles of buildings in urban planning in order to create neighborhoods with complementary heating and cooling demand profiles [20].

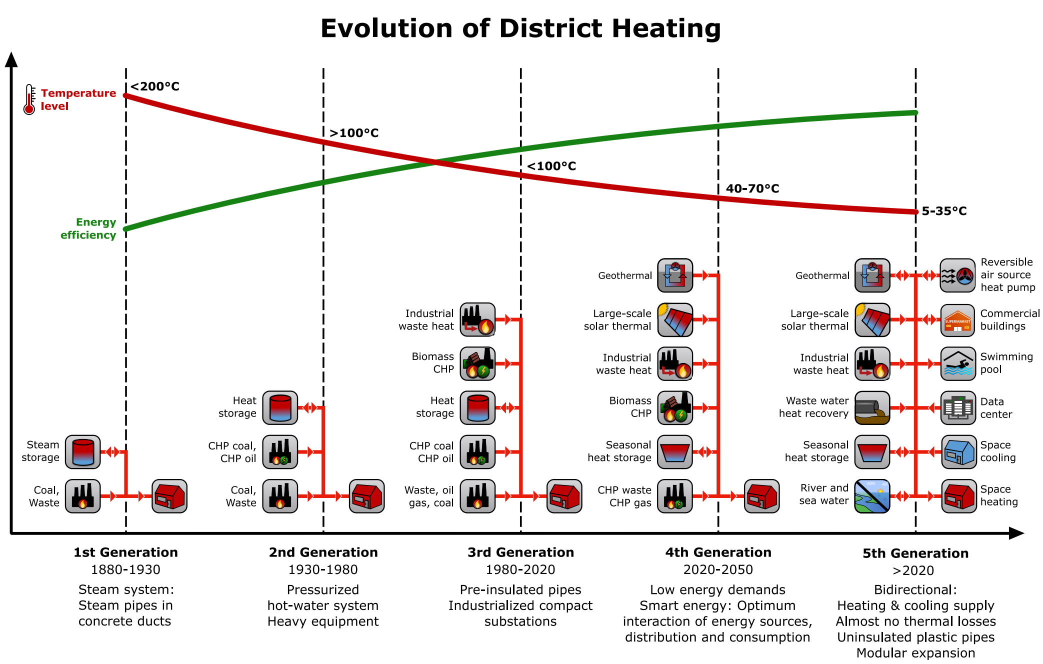

Figure 1: 5th Generation District Heating and Cooling networks are the latest stage in the evolution of district heating. Illustration based on Lund et al. [28].

1.1. Key metrics for quantifying waste heat potential

In this section, an overview about recently presented key metrics to quantify waste heat potential is provided: For data centers, Wahlroos et al. ([29],

[30]) present the *Energy Reuse Factor*, which describes the ratio of reused energy to total energy consumption for data centers.

Papapetrou et al. [31] introduce the *Waste Heat Fraction*. It is the ratio of waste heat potential to total heat consumption for a specific industrial sector and temperature band. However, their approach focuses on industrial processes for which waste heat sources and heating demands are usually not shifted by seasonal effects.

Fang et al. [5] discuss the potential of low temperature district heating networks for recovering industrial waste heat in northern China. For estimating the waste heat potential, they introduce the *Coefficient of Potential*, which describes the ratio of "theoretical amount of waste heat from all intensive sectors in district heating regions to district heating energy consumption". However, they do not elaborate this approach further regarding temporal availability or temperature levels of heat sources and demands.

Persson et al. [32] present key metrics to quantify heat recovery. They introduce the *Heat Recovery Rate* and *Heat Utilization Rate*. The heat recovery rate measures the proportion of recovered waste heat. The heat utilization rate indicates the extent to which recovered excess heat is actually used to cover heat demands.

Woolley et al. [33] consider the temporal distribution of waste heat in relation to the heat demand. For this purpose, they define an overlap function which describes the minimum of two exergy flows: The exergy flow of the (waste) heat source and the exergy flow of the heat sink. By integrating the overlap function over time, they calculate the total amount of exergy that can be recovered from the waste heat. Furthermore, they define a *Recovery*

Index as the ratio of recoverable exergy to total available exergy.

For BLTNs, no metric has yet been developed which quantifies the waste heat potential in these systems. However, Pass et al. [34] present the *Diversity index* to quantify the diversity of heating and cooling demands: A large Diversity index indicates that heating and cooling demands are about the same magnitude for a given point in time, which suggests that a large proportion of waste heat can be recovered. A Diversity index of zero indicates that only heating or only cooling demands occur at a given point in time and no waste heat can be recovered. The numeric value of the Diversity index has no physical meaning. In particular, no conclusions can be drawn about the proportion of balanced demands. Pass et al. consider exergy efficiency in order to evaluate the performance of a district energy system with BLTN. However, no conclusions about the profitability of the system, e.g. by considering total annualized costs, are drawn.

1.2. Contributions

In this paper, a novel metric is presented that quantifies the balancing potential of heating and cooling demands in districts with BLTN and at the same time characterizes the demand structure of a district. The metric is called *Demand Overlap Coefficient* (DOC), as it is a measure of the overlap of heating and cooling demand profiles. In contrast to the metrics presented in [5], [29], [30], [31] and [32], the DOC takes into account the simultaneity of heat sources and demands. Unlike the Diversity index presented in [34], the DOC has a physical meaning and can be interpreted intuitively: It describes the proportion of thermal demands that can potentially be balanced in a district energy system with BLTN. The DOC can be determined for different subsystems and indicates the balancing potential *inside* buildings or in the BLTN *between* buildings.

Based on 63 demand scenarios, correlations between the DOC and key performance indicators, like exergy efficiency and total annualized costs, are derived. The evaluation of the system performance is conducted with a linear program adapted from [35]. It is shown that the DOC can serve as a practical key metric to identify clusters of buildings with complementary heating and cooling demands and to estimate the profitability and efficiency of a BLTN in the early planning phase.

1.3. Paper organization

The structure of this paper is as follows: In Section 2.1, the DOC with all related equations is introduced. The methodology to evaluate the performance of a district energy system with BLTN is presented in Section 2.2. In Section 3, the DOC is determined for a real-world use case and the balancing of demands is explained in detail. In Section 4, 63 different demand scenarios are analyzed and correlations between the DOC and key performance indicators are derived. Finally, conclusions are provided in Section 5.

2. Methodology

In the following Section 2.1, the definitions and equations of the DOC are derived. The methodology for evaluating the performance of district energy systems with BLTNs is explained in Section 2.2.

2.1. Demand Overlap Coefficient

In urban districts, low temperature waste heat often results from cooling applications (e.g. space cooling with compression chillers). This low-grade waste heat can be directly fed into a BLTN to cover heating demands of other buildings. This way, heating and cooling demands are balanced out to some extent. The proportion of heating demands that can be covered by waste heat sources depends on the amount and temperature level of the waste heat but also on the simultaneity of demands and sources. In this section, the DOC is introduced to evaluate the waste heat potential for districts with BLTN. More precisely, the DOC describes the proportion of heating and cooling demands that can be canceled out in the system. In the following Section 2.1.1, the *District DOC* is introduced which characterizes the demand structure of a district. In the subsequent Sections 2.1.2 and 2.1.3, two further DOCs for demand balancing *inside* and *between* buildings are derived. Section 2.1.4 presents the relationships between all three DOCs.

2.1.1. District DOC

The District DOC is a metric to quantify the temporal correspondence of heating and cooling demands in a district, i.e. to what extend heating and cooling demands match in time and magnitude. The District DOC is calculated solely on the basis of building energy demands and no knowledge about the energy system is required. Fig. 2 shows exemplary heating and cooling demand profiles ($\dot{Q}_{\mathrm{h,dem}}(t)$ / $\dot{Q}_{\mathrm{c,dem}}(t)$). The balancing heat flow (that results from the cooling process and covers a proportion of the heating demand) is

$$\dot{Q}_{\mathrm{bal}}(t) = \min\left\{\dot{Q}_{\mathrm{h,dem}}(t), \dot{Q}_{\mathrm{c,dem}}(t)\right\} \tag{1}$$

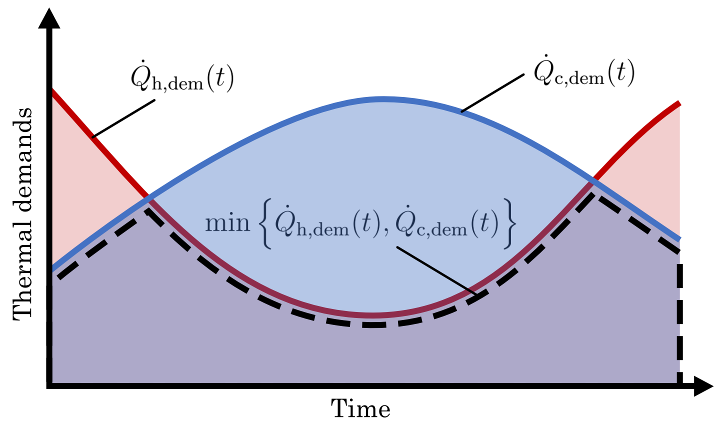

Figure 2: Heating (red) and cooling demands (blue) are depicted over time. The Demand Overlap Coefficient quantifies the overlap of both demands expressed by $\min\left\{\dot{Q}_{\mathrm{h,dem}}(t), \dot{Q}_{\mathrm{c,dem}}(t)\right\}$ (black dashed line).

and is indicated by the dashed black line in Fig. 2. The proportion of the balanced heating and cooling demands for one point in time t is

$$\frac{2 \cdot \min\left\{\dot{Q}_{\mathrm{h,dem}}(t), \dot{Q}_{\mathrm{c,dem}}(t)\right\}}{\dot{Q}_{\mathrm{h,dem}}(t) + \dot{Q}_{\mathrm{c,dem}}(t)} \tag{2}$$

Here, the factor 2 takes into account that one unit of balanced demands equals one unit of heating plus one unit of cooling demand, and thus ensures that the proportion ranges between 0 and 1. For an exemplary heating demand of $\dot{Q}_{\mathrm{h,dem}} = 6$ kW and a cooling demand of $\dot{Q}_{\mathrm{c,dem}} = 2$ kW, this proportion is

$$\Phi = \frac{4}{6+2} = \frac{1}{2} \tag{3}$$

The proportion of the total balanced demands during a time interval is

$$\Phi = \frac{\int 2 \cdot \min\left\{\dot{Q}_{\mathrm{h,dem}}(t), \dot{Q}_{\mathrm{c,dem}}(t)\right\} \mathrm{d}t}{\int \dot{Q}_{\mathrm{h,dem}}(t) + \dot{Q}_{\mathrm{c,dem}}(t)\ \mathrm{d}t} \tag{4}$$

and is therefore two times the area under the dashed line divided by the sum of the areas under the red and blue line. For discrete, equally spaced time intervals $t \in T$ follows:

$$\Phi = \frac{2 \cdot \sum_{t \in \mathrm{T}} \min \left\{ \dot{Q}_{\mathrm{h,dem},t}, \dot{Q}_{\mathrm{c,dem},t} \right\}}{\sum_{t \in \mathrm{T}} \left(\dot{Q}_{\mathrm{h,dem},t} + \dot{Q}_{\mathrm{c,dem},t} \right)} \tag{5}$$

By summing up all heating and cooling demands of all buildings $b \in B$ in a district, the definition of the District DOC is obtained:

$$\boxed{\Phi_{\mathrm{distr}} = \frac{2 \cdot \sum_{t \in \mathrm{T}} \min \left\{ \sum_{b \in \mathrm{B}} \dot{Q}_{\mathrm{h,dem},b,t}, \sum_{b \in \mathrm{B}} \dot{Q}_{\mathrm{c,dem},b,t} \right\}}{\sum_{t \in \mathrm{T}} \sum_{b \in \mathrm{B}} \left(\dot{Q}_{\mathrm{h,dem},b,t} + \dot{Q}_{\mathrm{c,dem},b,t} \right)}} \tag{6}$$

The DOC ranges between 0 and 1. A DOC of 0 means that heating and cooling demand profiles do not overlap at all, a DOC of 1 means they match exactly. However, the District DOC only estimates the demand balancing potential due to the fact that the temperature level of waste heat from chillers is usually not high enough to cover heating demands directly. As a result, in districts with BLTN, heat pumps and chillers are installed to raise or lower the temperature of waste heat flows. Therefore, in the following Section 2.1.2, this effect is taken into account when the DOC for a building energy system is derived.

2.1.2. Building energy system DOC (BES DOC)

The building energy system DOC (BES DOC) describes the balancing potential for a building energy system (BES) in which heating and cooling demands overlap. In the following, a BES with a heat pump and a chiller is considered. However, the definition of the BES DOC can be applied to any

BES configuration which use heat and cold from a thermal network. (For other BES configurations, Eqs. (7) and (8) have to be adapted to express the net heating and cooling demand of the BES). In Fig. 3, the considered BES with heat pump and chiller as well as the heating and cooling demands of the buildings ($\dot{Q}_{\text{h,dem},b,t}$ and $\dot{Q}_{\text{c,dem},b,t}$) are illustrated. The heat flow to the evaporator of the heat pump (or more general the heat demand of the BES) is denoted by $\dot{Q}_{\text{h,BES},b,t}$ and waste heat from the compression chiller (cooling demand of the BES) by $\dot{Q}_{\text{c,BES},b,t}$. These heat flows can be expressed with their respective COPs:

$$\dot{Q}_{\text{h,BES},b,t} = \dot{Q}_{\text{h,dem},b,t} \left(1 - \frac{1}{COP_{\text{HP}}}\right) \tag{7}$$

$$\dot{Q}_{\text{c,BES},b,t} = \dot{Q}_{\text{c,dem},b,t} \left(1 + \frac{1}{COP_{\text{CC}}}\right) \tag{8}$$

Waste heat from the chiller is used as heat source for the heat pump. This balancing heat flow is

$$\dot{Q}_{\text{BES,bal},b,t} = \min\left\{\dot{Q}_{\text{h,BES},b,t}, \dot{Q}_{\text{c,BES},b,t}\right\} \tag{9}$$

As a result, the BES DOC for the a building b is

$$\boxed{\Phi_{\text{BES},b} = \frac{2 \cdot \sum_{t\in\text{T}} \min\left\{\dot{Q}_{\text{h,BES},b,t}, \dot{Q}_{\text{c,BES},b,t}\right\}}{\sum_{t\in\text{T}} \left(\dot{Q}_{\text{h,BES},b,t} + \dot{Q}_{\text{c,BES},b,t}\right)} \quad \forall\, b \in \text{B}} \tag{10}$$

and describes proportion of balanced heating and cooling demands in a building. The BES DOCs of a set of buildings can be averaged and expressed by a mean BES DOC:

$$\boxed{\overline{\Phi}_{\text{BES}} = \frac{2 \cdot \sum_{b\in\text{B}} \sum_{t\in\text{T}} \min\left\{\dot{Q}_{\text{h,BES},b,t}, \dot{Q}_{\text{c,BES},b,t}\right\}}{\sum_{b\in\text{B}} \sum_{t\in\text{T}} \left(\dot{Q}_{\text{h,BES},b,t} + \dot{Q}_{\text{c,BES},b,t}\right)}} \tag{11}$$

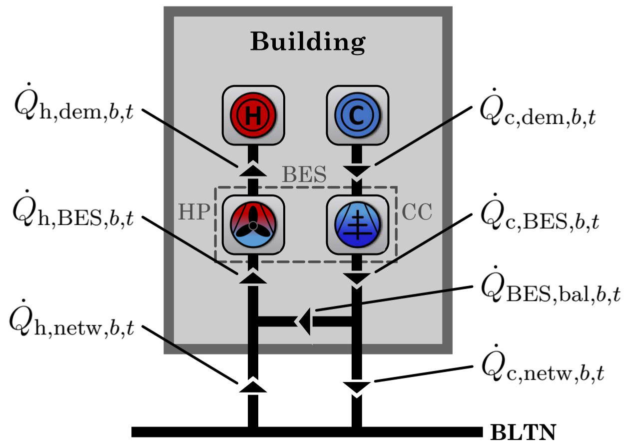

Figure 3: Demand balancing in buildings: Waste heat from the compression chiller (CC) is used as heat source for the heat pump (HP). Residual loads are taken from the thermal network ($\dot{Q}_{\mathrm{h,netw},b,t}$ and $\dot{Q}_{\mathrm{c,netw},b,t}$).

Equivalently, the mean BES DOC ($\overline{\Phi}_{\mathrm{BES}}$) can be expressed with the BES DOCs of the individual buildings ($\Phi_{\mathrm{BES},b}$):

$$\overline{\Phi}_{\mathrm{BES}} = \frac{\sum_{b\in\mathrm{B}}\left(\Phi_{\mathrm{BES},b}\sum_{t\in\mathrm{T}}\left(\dot{Q}_{\mathrm{h,BES},b,t}+\dot{Q}_{\mathrm{c,BES},b,t}\right)\right)}{\sum_{b\in\mathrm{B}}\sum_{t\in\mathrm{T}}\left(\dot{Q}_{\mathrm{h,BES},b,t}+\dot{Q}_{\mathrm{c,BES},b,t}\right)} \tag{12}$$

2.1.3. Network DOC

The Network DOC is a measure for the overlap of the heat flows from the network to the buildings and vice versa and therefore describes the balancing of heating and cooling demands between buildings. In Fig. 3, the heat flow from the BLTN to the building is

$$\dot{Q}_{\mathrm{h,netw},b,t} = \dot{Q}_{\mathrm{h,BES},b,t} - \dot{Q}_{\mathrm{BES,bal},b,t} \tag{13}$$

and from the building to the BLTN is

$$\dot{Q}_{\mathrm{c,netw},b,t} = \dot{Q}_{\mathrm{c,BES},b,t} - \dot{Q}_{\mathrm{BES,bal},b,t} \tag{14}$$

For the Network DOC, these net demands of all buildings (heating demand: $\sum_{b \in \mathrm{B}} \dot{Q}_{\mathrm{h,netw},b,t}$; cooling demand: $\sum_{b \in \mathrm{B}} \dot{Q}_{\mathrm{c,netw},b,t}$) are considered. The Network DOC is then defined as

$$\boxed{\Phi_{\mathrm{netw}} = \frac{2 \cdot \sum_{t \in \mathrm{T}} \min \left\{ \sum_{b \in \mathrm{B}} \dot{Q}_{\mathrm{h,netw},b,t}, \sum_{b \in \mathrm{B}} \dot{Q}_{\mathrm{c,netw},b,t} \right\}}{\sum_{t \in \mathrm{T}} \left(\sum_{b \in \mathrm{B}} \dot{Q}_{\mathrm{h,netw},b,t} + \sum_{b \in \mathrm{B}} \dot{Q}_{\mathrm{c,netw},b,t} \right)}} \tag{15}$$

Demands, which cannot be balanced in the BLTN, are covered by external supply systems, e.g. an energy hub (EH). In the following, these residual demands of the network are denoted by $\dot{Q}_{\mathrm{h,EH},t}$ and $\dot{Q}_{\mathrm{c,EH},t}$.

2.1.4. Relationship between different DOCs

In this section, the DOCs are summarized and it is shown how they are related to each other. The definitions of the District DOC, BES DOC and Network DOC are illustrated in Fig. 4. The BES DOC and Network DOC couple the thermal demands of the different subsystems with each other: The net heating and cooling demands of building b are coupled with the thermal demands of the BES by the BES DOC:

$$\sum_{t \in \mathrm{T}} (\dot{Q}_{\mathrm{h,netw},b,t} + \dot{Q}_{\mathrm{c,netw},b,t}) = (1 - \Phi_{\mathrm{BES},b}) \sum_{t \in \mathrm{T}} (\dot{Q}_{\mathrm{h,BES},b,t} + \dot{Q}_{\mathrm{c,BES},b,t}) \tag{16}$$

Likewise, the net building demands and the residual network demands are coupled by the Network DOC:

$$\sum_{t \in \mathrm{T}} (\dot{Q}_{\mathrm{h,EH},t} + \dot{Q}_{\mathrm{c,EH},t}) = (1 - \Phi_{\mathrm{netw}}) \sum_{b \in \mathrm{B}} \sum_{t \in \mathrm{T}} (\dot{Q}_{\mathrm{h,netw},b,t} + \dot{Q}_{\mathrm{c,netw},b,t}) \tag{17}$$

By inserting Eq. (16) in Eq. (17), an expression is obtained that couples the thermal demands of the BESs with the residual network demands:

$$\sum_{t \in \mathrm{T}} (\dot{Q}_{\mathrm{h,EH},t} + \dot{Q}_{\mathrm{c,EH},t}) = (1 - \Phi_{\mathrm{netw}})(1 - \overline{\Phi}_{\mathrm{BES}}) \sum_{b \in \mathrm{B}} \sum_{t \in \mathrm{T}} (\dot{Q}_{\mathrm{h,BES},b,t} + \dot{Q}_{\mathrm{c,BES},b,t}) \tag{18}$$

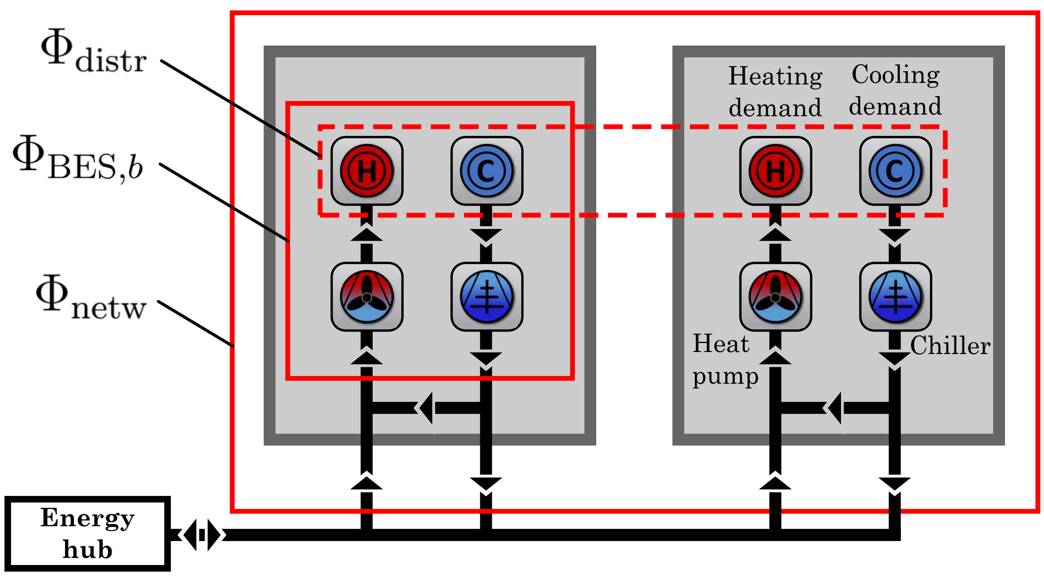

Figure 4: The simultaneity of heating and cooling demands can be calculated for three subsystems: Cumulated demands of all connected buildings (Φ_{distr}), demands of an individual building energy system ($\Phi_{\mathrm{BES},b}$) and cumulated net demand of all connected buildings (Φ_{netw}).

In Section 4, it is shown that a correlation between the Network DOC, mean BES DOC and District DOC exists, from which the approximation

$$(1-\Phi_{\text{netw}})(1-\overline{\Phi}_{\text{BES}}) \approx (1-\Phi_{\text{distr}}) \tag{19}$$

is derived.

2.1.5. Limitations

The definition of the DOC is subject to simplifications: A limitation of the Network DOC is that the spatial distribution of heat sources and sinks is not taken into account, and therefore hydraulic network limitations are neglected. As a result, an ideal exchange of waste heat among buildings is assumed. This simplification is considered justified for small districts. However, for large thermal networks with a large number of connected buildings, the effect of hydraulic limitations becomes more relevant. Moreover, by assuming an ideal exchange of waste heat, heat losses to the ground are neglected.

The Network DOC is particularly meaningful for systems with no or only small storage capacities. For systems with large thermal storages, like seasonal storages, the simultaneity of demands is of less relevance since storages enable demand balancing across different time periods. If thermal storages are used in the network, the temporal resolution of the periods for calculating the Network DOC should be adjusted to the storage capacity. For example, if thermal storages balance day-night cycles, the calculation of the Network DOC should be based on time periods with a length of one day. Similarly, the thermal inertia of the water mass in the network can function as a thermal storage. However, this effect can be neglected for most of the BLTNs since the water volume of the network is small, especially compared to the water volume of a central storage.

2.1.6. Application in planning of BLTNs

The DOC is a metric to support the development of sustainable urban districts, and especially the planning of district energy systems with BLTNs. In an early design phase of districts, urban planners can use the DOC to ensure that the waste heat potential of a district can be exploited to the greatest extend possible. In this context, the DOC can help to answer questions like:

- Which building types are considered for a district and what is a beneficial composition from an energy point of view? Only dwellings or also commercial buildings? If only dwellings are planned, a BLTN tends to be less profitable since waste heat and heat demands do not occur simultaneously.

- How are different buildings grouped in a district, e.g. mixed-use zones or homogeneous structure? Mixed-use zones lead to smaller clusters with complementary demands which can be interconnected with small networks.

In the technical planning process of a BLTN, the DOC is a practical metric to answer questions like:

- Should a more distant building connected to the network or should it be supplied by an individual energy system?

- Is it beneficial to connect buildings outside of the district to the BLTN? For example, connecting a nearby supermarket or factory offering waste heat in winter can be beneficial for the overall system performance.

- Should different BLTNs in a city be connected or stay seperated? To answer this question, the DOC can be calculated with the cumulated demands of both BLTN clusters. A connection of two BLTNs can be beneficial if the DOC of the connected clusters is larger than the DOC of the single clusters.

2.2. Evaluation of system performance

In Section 4, correlations between the DOCs and the performance of district energy systems with BLTN are investigated. In order to determine the system performance for many different use cases, an optimization model (linear programming) is used. The model is briefly explained in the following Section 2.2.1. In Section 2.2.2, the key performance indicators for the evaluations in this study are introduced.

2.2.1. Linear program for system calculation

The linear program used in this study is adapted from a model presented by Wirtz et al. [35]. The linear program determines the optimal selection and sizing of all system components as well as their optimal operation by minimizing total annualized costs. The optimization model is described by two superstructures: one for the energy hub and one for the building energy systems. From the technologies of the superstructure, the optimal system configuration is selected in the optimization.

The superstructure of the energy hub is depicted in Fig. 5. It contains a reversible air source heat pump which heats or cools the BLTN. The COP of the heat pump is calculated a priori based on the ambient air temperature. As storage units, an ice thermal energy storage (ITES) and a battery (BAT)

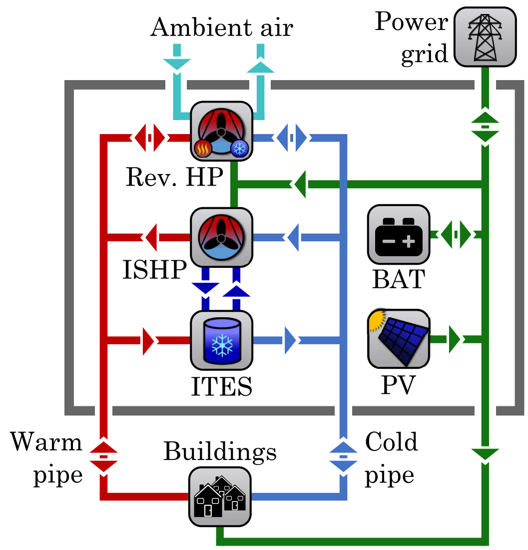

Figure 5: Optimization superstructure of the energy hub: Heat is generated by a reversible air source heat pump (Rev. HP) and the ice storage heat pump (ISHP). The ice thermal energy storage (ITES) and reversible heat pump can cool the thermal network. Photovoltaic modules (PV) generate electricity. A battery (BAT) can be installed to increase the self consumption rate.

are considered. Surplus heat from the BLTN can be used to regenerate the ice storage. A heat pump connected to the ice storage (ISHP) can extract heat from the storage and heat the BLTN. For the water in the ice storage, a constant temperature of 0 °C is assumed. Furthermore, photovoltaic modules (PV) are part of the superstructure. The superstructure of the building energy systems is depicted in Fig. 6. It contains a heat pump, electric boiler, heat storage, chiller and a heat exchanger for direct cooling. The objective function and all constraints of the linear program are listed in Appendix B.

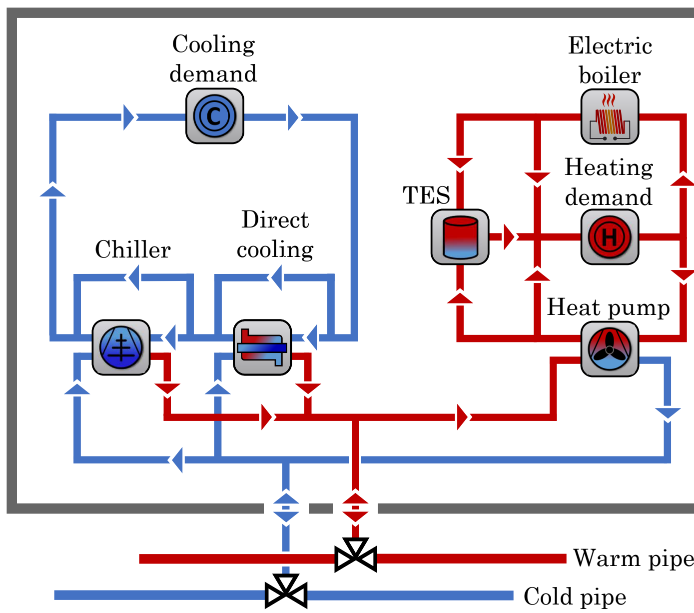

Figure 6: Optimization superstructure of building energy systems (based on [35]): Heating demands are covered by a water-to-water heat pump, electric boiler and thermal energy storage (TES). Cooling demands are covered by a compression chiller and a heat exchanger for direct cooling with the cold pipe of the BLTN.

2.2.2. Key performance indicators

Based on the system operation (determined with the linear program), four key performance indicators (KPIs) are considered in this study which are introduced in the following.

Specific supply costs for heating and cooling

The objective function of the optimization model are total annualized costs (TAC). The specific costs for the heating and cooling supply are

$$c_{\text{tot}} = \frac{TAC}{Q^{\text{tot}}_{\text{h,dem}} + Q^{\text{tot}}_{\text{c,dem}}} \quad \text{in} \quad \frac{\text{EUR}}{\text{MWh}} \tag{20}$$

in which $Q^{\text{tot}}_{\text{h,dem}}/Q^{\text{tot}}_{\text{c,dem}}$ are the annual heating and cooling demands.

Exergy efficiency

Following the exergetic assessment of districts in [36] and [37], the exergy efficiency is used as another KPI. The exergy efficiency of a system is the ratio of total useful exergy to the total exergy expenditures:

$$\eta_{\text{ex}} = \frac{E^{\text{tot}}_{\text{h,dem}} + E^{\text{tot}}_{\text{c,dem}} + W^{\text{tot}}_{\text{feed-in}}}{W^{\text{tot}}_{\text{grid}} + W^{\text{tot}}_{\text{PV}}} \tag{21}$$

Here, $E^{\text{tot}}_{\text{h,dem}}/E^{\text{tot}}_{\text{c,dem}}$ denote the exergy of the annual heating and cooling demands of all buildings. The total electricity fed into the electricity grid ($W^{\text{tot}}_{\text{feed-in}}$) is considered useful exergy, the total electricity imported from the grid ($W^{\text{tot}}_{\text{grid}}$) is considered expenditure. The electricity generated by photovoltaics is considered expenditure ($W^{\text{tot}}_{\text{PV}}$). Based on [38], the exergy of heat and cold flows is:

$$E_{\mathrm{h,dem}}^{\mathrm{tot}} = Q_{\mathrm{h,dem}}^{\mathrm{tot}} \left(1 - \frac{T_{\mathrm{ref}}}{T_{\mathrm{h,sup}}}\right) \tag{22}$$

$$E_{\mathrm{c,dem}}^{\mathrm{tot}} = Q_{\mathrm{c,dem}}^{\mathrm{tot}} \left(\frac{T_{\mathrm{ref}}}{T_{\mathrm{c,sup}}} - 1\right) \tag{23}$$

Here, the $T_{\mathrm{h,sup}}/T_{\mathrm{c,sup}}$ denote the supply temperature of the heating/cooling system in the building and T_{ref} denotes the reference temperature (in this study: $T_{\mathrm{ref}} = 25\,^{\circ}\mathrm{C} = 298.15\,\mathrm{K}$).

System COP

The entire energy supply system with the reversible heat pump in the energy hub and the heat pumps in the buildings can be considered as one cascaded heat pump process. Therefore, as a third KPI, an overall coefficient of performance of the energy supply system (*System COP*) is considered. The definition is based on the *Figure of merit* introduced by Rosen et al. [39]:

$$COP_{\mathrm{Sys}} = \frac{Q_{\mathrm{h,dem}}^{\mathrm{tot}} + Q_{\mathrm{c,dem}}^{\mathrm{tot}} + W_{\mathrm{feed-in}}^{\mathrm{tot}}}{W_{\mathrm{grid}}^{\mathrm{tot}} + W_{\mathrm{PV}}^{\mathrm{tot}}} \tag{24}$$

Here, $Q_{\mathrm{h,dem}}^{\mathrm{tot}}$ and $Q_{\mathrm{c,dem}}^{\mathrm{tot}}$ denote the total heating and cooling demands, $W_{\mathrm{feed-in}}^{\mathrm{tot}}$ the total electricity fed into the electricity grid, $W_{\mathrm{grid}}^{\mathrm{tot}}$ the total electricity imported from the grid and $W_{\mathrm{PV}}^{\mathrm{tot}}$ the total PV generation.

Specific CO_2 emissions

The specific CO_2 emissions of the district energy system are

$$e_{\mathrm{tot}} = \frac{W_{\mathrm{grid}}^{\mathrm{tot}} e_{\mathrm{grid}}}{Q_{\mathrm{h,dem}}^{\mathrm{tot}} + Q_{\mathrm{c,dem}}^{\mathrm{tot}}} \quad \text{in} \quad \frac{\mathrm{t}_{\mathrm{CO_2}}}{\mathrm{MWh}} \tag{25}$$

Here, e_{grid} is the CO_2 factor of the electricity grid mix.

2.2.3. *Reference system*

In order to evaluate the performance of the BLTN system, it is compared with a reference system which represents a state-of-the-art solution. For heating and cooling supply in the reference system, each building is equipped with an air source heat pump, electric boiler, heat storage as well as a compression chiller. Like in the BLTN system, PV modules are installed. The reference system does not have an energy hub or thermal network, and therefore heat exchange between buildings is not possible.

3. Use case

In this section, the presented methodology is applied to a real-world use case. Section 3.1 provides a brief description of the use case. In Section 3.2, the performance of the system is evaluated according to four KPIs and compared to a reference system. In Section 3.3, the three DOCs are determined for the use case and the effect of demand balancing is described in detail.

3.1. *Use case description*

The use case (adopted from [35]) is a reasearch campus in Germany, for which 17 buildings are considered. A monitoring system has been installed on the campus, which logs heating and cooling demands at substations in all buildings with a sub-hourly resolution. For this study, raw data for one year has been aggregated to hourly demand time series (8760 data points for each demand profile). An overview of heating and cooling demands of the buildings provides Fig. 7. Here, all 17 buildings are grouped into 6 building clusters (A $-$ F). The building clusters are used in the investigations in Section 4. Buildings 1 and 2, a laboratory and a canteen, have the

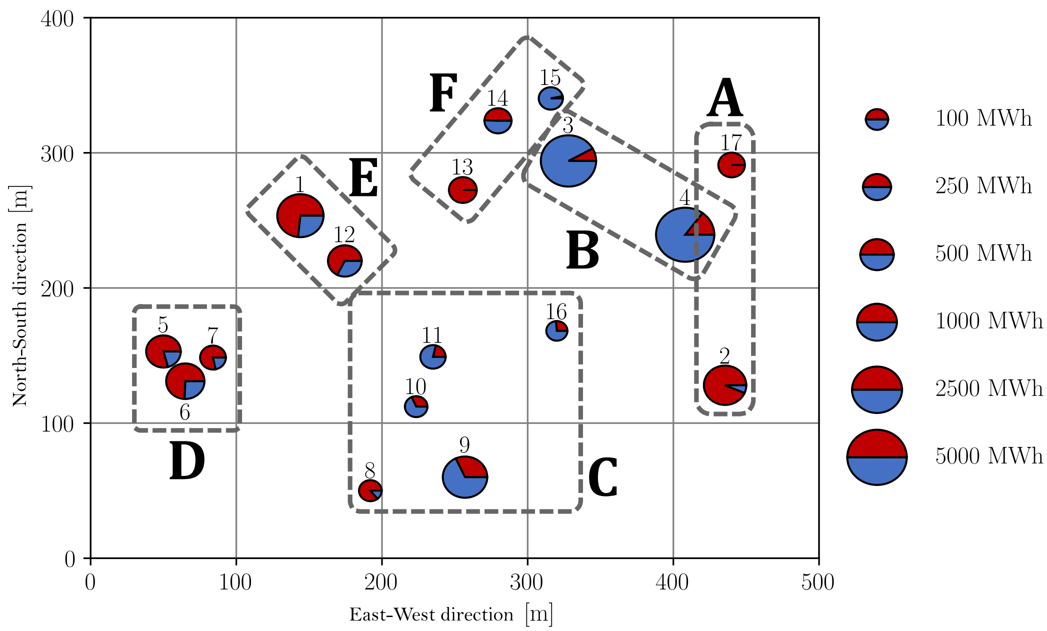

Figure 7: Total annual heating (red) and total annual cooling demand (blue) for 17 buildings on the research campus including two data centers (building 3 and 4). The building clusters A − F are used for generating different demand scenarios in Section 4. Illustration adapted from [35].

largest heating demands. These two buildings account for 49 % of the heating demand (total heating demand: 6.36 GWh). Buildings 3 and 4 are data centers, which account for 73 % of the cooling demand (total cooling demand: 10.0 GWh). Detailed building information is provided in Table A.4 in the Appendix. For the heating and cooling systems of the buildings, constant supply temperatures of $T_{\mathrm{h,sup}} = 60\,°\mathrm{C}$ and $T_{\mathrm{c,sup}} = 16\,°\mathrm{C}$ are assumed.

3.2. System evaluation

Based on the operation of the BLTN system, the four KPIs introduced in Section 2.2.2 are evaluated. The optimal configuration of the BLTN system (determined with the linear program) is described in Appendix C. The key performance indicators for the BLTN system and the reference system are listed in Table 1 (data obtained from the optimization results). The specific supply costs of the BLTN solution are 37.6 EUR/MWh. The supply costs of the reference system are 11.9 % higher (42.1 EUR/MWh). Moreover, the BLTN system performs substantially better from a thermodynamic perspective: The exergy efficiency is 33.5 %, and thus 6.8 percentage points higher compared to the reference system. The System COP of the BLTN system is 5.01, which means that with one unit of electric power 5 units of heating or cooling demand can be supplied. As a result of the higher efficiency, the CO_2 emissions of the BLTN system are lower (64.8 g/kWh) compared to the reference system (92.4 g/kWh).

Table 1: Comparison of KPIs of the system with BLTN and the reference system calculated based on the optimization results.

KPI	Unit	BLTN	Reference	
Specific supply costs	EUR/MWh	37.6	42.1	(+ 11.9 %)
Exergy efficiency	—	33.5 %	26.7 %	(− 6.8 p.p.)
System COP	—	5.01	3.95	(− 1.06)
Specific CO_2 emissions	g/kWh	64.8	92.4	(+ 42.6 %)

3.3. Demand balancing

Based on (measured) heating and cooling demand profiles of all 17 buildings, the District DOC is calculated to $\Phi_{\text{distr}} = 0.632$ (Eq. (6)). The cumulated thermal demands in different parts of the energy system are depicted in Fig. 8. The total heating and cooling demands of the buildings are 6359 MWh and 10042 MWh, respectively, which is illustrated in the left column in Fig. 8 a). The cumulated thermal demands of the building energy systems (obtained from the optimization results) are illustrated in the second column: The heating demands of the building energy systems are lower (4556 MWh) than the original heating demands (6359 MWh) since the heat flow to the evaporator of heat pumps is smaller than the outgoing heat flow at the condenser. Furthermore, the operation of electric boilers lower the thermal demands of the BESs. The cooling demand (10042 MWh) remains the same since all cooling energy is provided by direct cooling (heat exchangers). Heating and cooling demands of BESs overlap and can be balanced to some extent: The proportion of balanced demands in buildings is expressed by the BES DOC (Eq. (10)). The BES DOCs of the 17 buildings (obtained from the optimization results) are listed in Table 2. They range between 0 and 0.52. The largest BES DOC is obtained in building 14, in which the cooling demand almost equals the heating demand, and thus more than half of the thermal demands are balanced in the building. Buildings 13 and 17 do not have a cooling demand and therefore no balancing takes place ($\Phi_{\mathrm{BES},13} = \Phi_{\mathrm{BES},17} = 0$).

Table 2: Building energy system DOCs (Φ_{BES}) of all 17 buildings based on optimization results.

Building	1	2	3	4	5	6	7	8	9
Φ_{BES}	0.41	0.06	0.12	0.22	0.31	0.45	0.27	0.20	0.50
Building	10	11	12	13	14	15	16	17	
Φ_{BES}	0.24	0.33	0.45	0	0.52	0.05	0.37	0	

Based on Eq. (11), a mean BES DOC of $\overline{\Phi}_{\mathrm{BES}} = 0.251$ is obtained and

3668 MWh are balanced in buildings (c.f. Fig. 8 a)). As a result, the remaining heating demand, which is covered by the BLTN, is 2722 MWh and the cooling demand 8208 MWh. The sum of the remaining heating and cooling demands is

$$14598\,\text{MWh} \cdot (1 - \overline{\Phi}_{\text{BES}}) = 10930\,\text{MWh} \tag{26}$$

as illustrated in Fig. 8 (b).

The proportion of demands that is balanced in the BLTN is quantified by the Network DOC. With Eq. (15), the Network DOC is calculated to $\Phi_{\text{netw}} = 0.457$ (based on the optimization results). Due to network balancing, the heating demand that needs to be covered by the energy hub is further reduced from 2722 MWh to 224 MWh. Accordingly, the cooling demand covered by the energy hub is reduced from 8208 MWh to 5710 MWh, as shown in Fig. 8 a). The sum of the heating and cooling demands which needs to be covered by the energy hub is then

$$10930\,\text{MWh} \cdot (1 - \Phi_{\text{netw}}) = 5934\,\text{MWh} \tag{27}$$

In this balance, heat losses (or gains) of the network are neglected since they play a minor role: The net heat loss of the warm pipe is 6 MWh and the net thermal loss of the cold pipe is 29 MWh.

3.3.1. Balancing over the course of the year

The DOC is an aggregated metric which does not reveal any information about the temporal distribution of the demand balancing. To investigate the temporal distribution, the demand balancing is illustrated for the considered year in Fig. 9. The cumulated demands of the district (measured data) are depicted Fig. 9 a): The cooling demand occurs throughout the year and

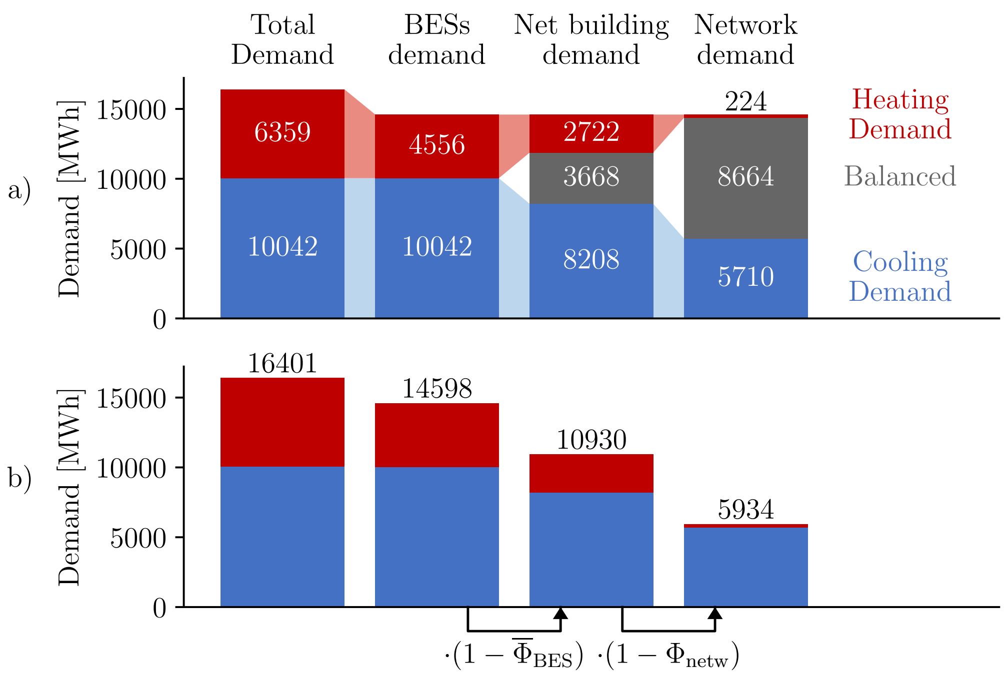

Figure 8: Subfigure a) illustrates from left to right: The total heating and cooling demands of all buildings in the district (6359 MWh/10042 MWh); the thermal demands of the building energy systems (BESs); the thermal demand transferred from the BLTN to the buildings (3668 MWh are balanced in buildings); the residual demand of the BLTN that is covered by the energy hub (4996 MWh are balanced in the BLTN). Subfigure b) illustrates the sum of the heating and cooling demands depicted in Subfigure a).

reaches its peak in summer. The heating demand predominantly occurs during winter months. A small heating demand occurs also during summer. In Fig. 9 b), the thermal demands of the BESs (based on the optimization results) are illustrated (denoted by $\dot{Q}_{\mathrm{h,BES},b,t}/\dot{Q}_{\mathrm{c,BES},b,t}$ in Fig. 3). The change of the heating demands from Fig. 9 a) to b) results from heat pumps as well as the electric boilers and heat storages in the BESs (balancing not yet included): The heat demand of the BESs is lower since the heat flow at the evaporator of heat pumps is lower than the outgoing heat flow at the condenser. Peak demands, e.g. in the second half of January, are shaved with electric boilers and thermal storages. The heating demand profile in Fig. 9 b) shows a maximum of 1.1 MW. In Fig. 9 c), the net demand of the buildings (after balancing in buildings) is depicted. The change of demands from Fig. 9 b) to c) is due to the balancing in buildings. The peak heating demand is lowered from 1.1 to 0.8 MW and the peak cooling demand to 2.2 MW. Fig. 9 d) depicts the thermal demands which are not balanced in the network, and are covered by the energy hub. From Fig. 9 c) to d), the thermal demands reduce due to balancing between buildings. As illustrated in Fig. 8, the remaining heating demand is 224 MWh and the remaining cooling demand is 5710 MWh. Due to the balancing in buildings and network, heating demands are almost completely canceled out. The peak heating demand is reduced from 1.88 MW to 0.49 MW (−74 %) and the peak cooling demand (begin of July) is reduced from 2.43 MW to 2.25 MW (−7 %). During winter, heating and cooling demands are balanced out almost completely. During summer, a large residual cooling demand remains that is covered by the energy hub.

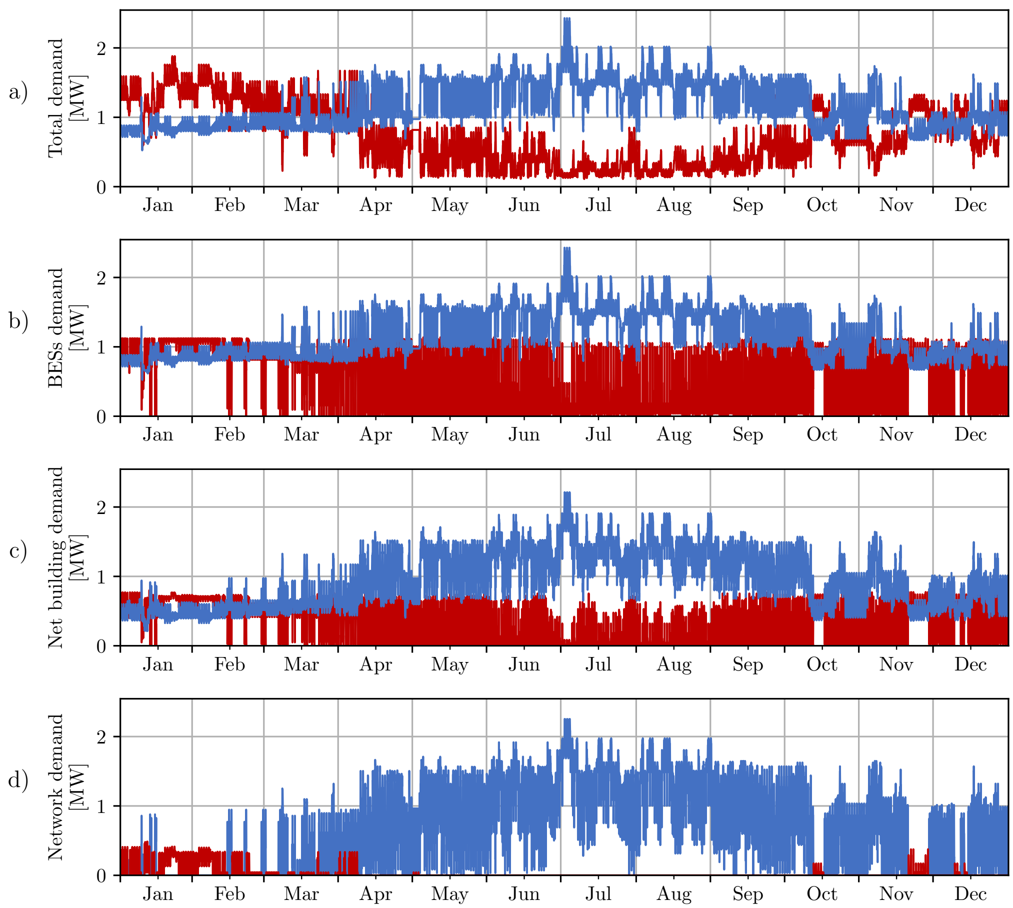

Figure 9: Cumulated heating and cooling demands of all buildings for one year: a) Total building demand (for space heating and cooling), b) thermal demand of building energy systems (BESs) before balancing in buildings, c) net building demands (after balancing in buildings), d) residual network demand that is covered by the enery hub (after balancing between buildings).

4. Correlation of DOC and key performance indicators

In this section, the performance and profitability of district energy systems with BLTN are related to the demand structure, especially the simultaneity of heating and cooling demands. In order to investigate this correlation, demand scenarios are derived from the real-world use case and for each of these scenarios the performance of a BLTN is evaluated. Section 4.1 presents the methodology for generating different demand scenarios. In Section 4.2, correlations between different DOCs are investigated. Section 4.3 presents correlations between the system performance and the demand structure as well as a comparison with the reference system.

4.1. Demand scenario generation

By selecting different subsets of buildings of the original use case (described in Section 3), a large variety of different demand scenarios is generated. For this purpose, the 17 buildings are aggregated into 6 building clusters (A, B, C, D, E, F), as depicted in Fig. 7. In Table 3, the demands of all building clusters are listed along with their District DOC. Furthermore, a heating-cooling ratio $R \in [-1, 1]$ is considered, which indicates whether heating or cooling demands are predominant in the district:

$$R = \frac{Q_{\text{h,dem}}^{\text{tot}} - Q_{\text{c,dem}}^{\text{tot}}}{Q_{\text{h,dem}}^{\text{tot}} + Q_{\text{c,dem}}^{\text{tot}}} \tag{28}$$

$R = 1$ indicates a scenario with only heating demands, $R = -1$ means only cooling demands are observed. If heating demands equal cooling demands, the demand ratio is $R = 0$.

Based on the 6 building clusters, $2^6 - 1 = 63$ non-empty cluster subsets can be selected. In each of the 63 subsets, different building clusters are

Table 3: Building clusters (A-F) used for demand scenario generation.

	Buildings	$\dot{Q}^{\mathrm{tot}}_{\mathrm{h,dem}}$	$\dot{Q}^{\mathrm{tot}}_{\mathrm{c,dem}}$	$\dot{Q}^{\mathrm{peak}}_{\mathrm{h,dem}}$	$\dot{Q}^{\mathrm{peak}}_{\mathrm{c,dem}}$	Φ_{distr}	R
		[MWh]	[MWh]	[MW]	[MW]	—	—
A	1, 12	1410	84	0.48	0.33	0.05	0.89
B	2, 17	987	7347	0.33	1.41	0.24	−0.76
C	3, 4	677	1336	0.28	0.41	0.61	−0.33
D	5, 6, 7	1233	377	0.37	0.15	0.38	0.53
E	8, 9, 10, 11, 16	1702	658	0.52	0.28	0.44	0.44
F	13, 14, 15	350	241	0.14	0.06	0.65	0.19

selected and, as a result, 63 different demand scenarios are considered. Each demand scenario has an individual demand structure and District DOC. The performance of a BLTN system is evaluated for each demand scenario with the optimization model introduced in Section 2.2.1.

4.2. Correlation between different DOCs

In this section, a correlation between the District DOC and the Network DOC/mean BES DOC is derived. The District DOC is calculated with the measured demand profiles, the Network DOC and mean BES DOC is obtained from the optimization results. In Fig. 10, the three DOCs are plotted for all 63 demand scenarios: The Network DOC is plotted against the mean BES DOC and the District DOC is indicated by the coloring. Except for one demand scenario, the Network DOC ranges between 0 and 0.5. Similarly, the mean BES DOC does not exceed 0.5. No correlation between the Network DOC and mean BES DOC is observed.

However, a correlation between the total share of balanced demands (ex-

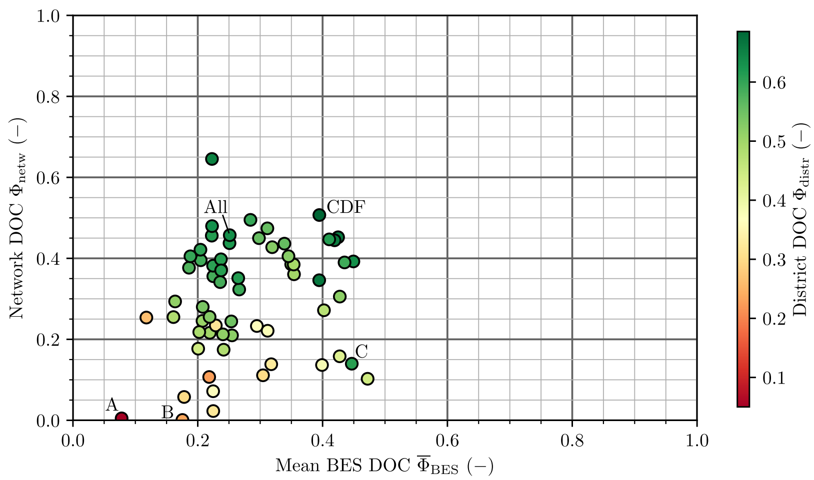

Figure 10: Illustration of the three Demand Overlap Coefficients: Network DOC, mean BES DOC and District DOC.

pressed with the mean BES DOC and Network DOC) and the District DOC is found, as illustrated in Fig. 11. On the horizontal axis, the product $(1-\Phi_{\mathrm{netw}})(1-\overline{\Phi}_{\mathrm{BES}})$ is plotted, which is the proportion of demands that cannot be balanced in buildings or BLTN (c.f. Eq. (18)). The term $(1-\Phi_{\mathrm{distr}})$ is plotted on the vertical axis. A distinctive correlation is observed, which shows that the total demand balancing (in buildings and network) can be derived approximately from the District DOC: $(1-\Phi_{\mathrm{netw}})(1-\overline{\Phi}_{\mathrm{BES}}) \approx (1-\Phi_{\mathrm{distr}})$. The District DOC Φ_{distr} is calculated solely with the building's heating and cooling demands (Eq. (6)) and no detailed knowledge about the system design or operation is required. Therefore, relations between the District DOC and the system performance are investigated in the following section.

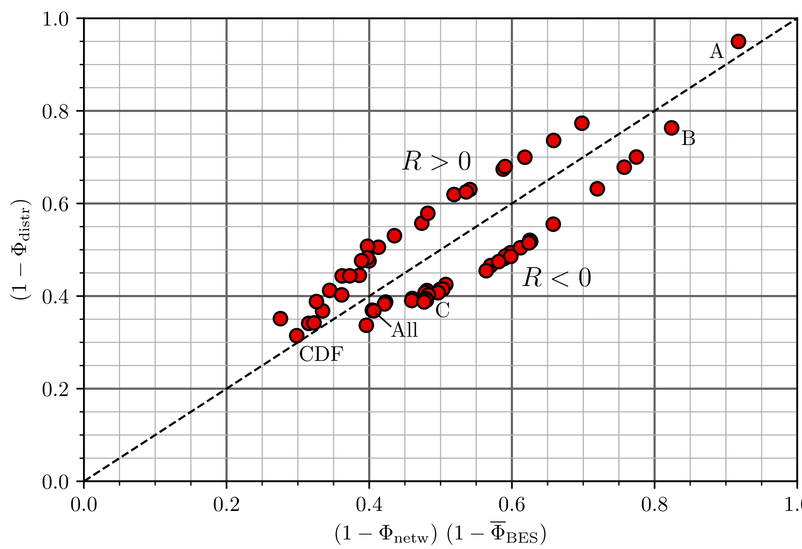

Figure 11: The share of thermal demands, that cannot be balanced in buildings or BLTN, i.e. $(1 - \Phi_{\mathrm{netw}})(1 - \overline{\Phi}_{\mathrm{BES}})$, correlates with the District DOC Φ_{distr}.

4.3. Correlation between system performance and District DOC

In this section, correlations between the District DOC and key performance indicators (obtained from optimization results) are investigated. In Fig. 12, the specific supply costs are plotted against the District DOC for all 63 demand scenarios. The color indicates the heating-cooling ratio R. The supply costs of demand scenarios with a larger heating than cooling demands ($R > 0$) decrease with increasing District DOC. The demand scenario, which is labeled *All*, comprises all building clusters and is therefore identical to the case study investigated in Section 3. The highest supply costs are observed in demand scenario A. In this scenario, heating demands dominate and almost no demand balancing takes place. For demand scenarios with larger District DOC, more and more waste heat is recovered (from buildings with

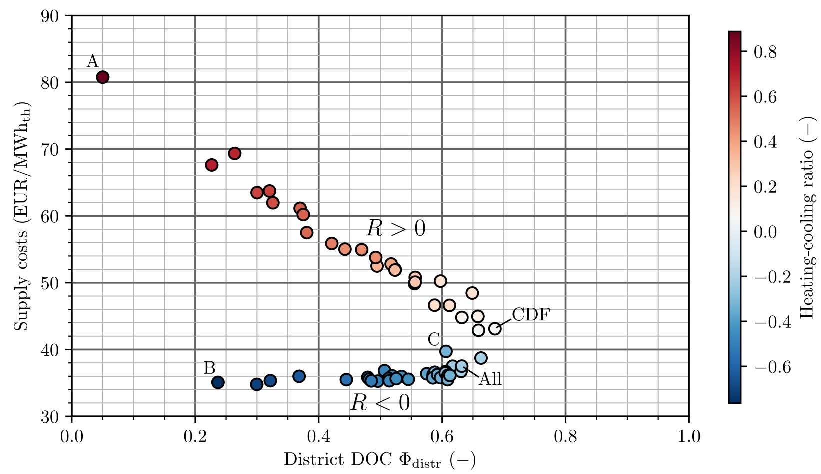

Figure 12: Specific heating and cooling supply costs of all 63 demand scenarios are plotted against the District DOC. The demand scenario comprising all building clusters is labeled *All*.

cooling demands). This reduces the operation of the reversible heat pump in the energy hub, and thus electricity costs. In Fig. 12, scenario CDF has the largest DOC ($\Phi_{\mathrm{distr}} \approx 0.65$) and the total heating and cooling demands are almost equal ($R \approx 0$). For demand scenarios in which cooling demands dominate, specific supply costs are almost constant. This is explained as follows: On the one hand, the lower the heating demands, the lower the specific supply costs, since cooling demands can be covered at lower costs than heating demands. (This results from the fact, that for direct cooling with the cold pipe of the BLTN no electricity is needed). On the other hand, the lower the heating demands, the higher the load of the reversible heat pump in the energy hub (in order to balance the residual cooling demands of the BLTN), which causes additional electricity costs. The two effects cancel each other out.

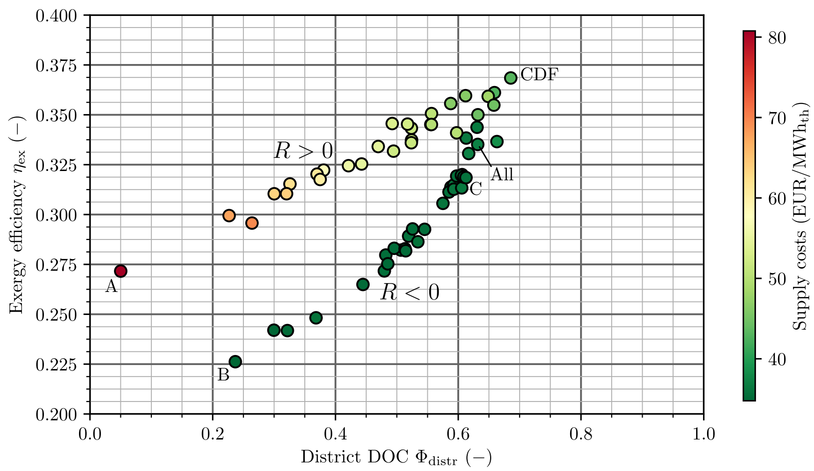

Figure 13: Exergy efficiency plotted against District DOC. The exergy efficiency correlates in both branches ($R > 0$ and $R < 0$) with the District DOC: Larger District DOCs result in higher exergy efficiencies.

In Fig. 13, the exergy efficiency is plotted against the District DOC for all demand scenarios. Similar to Fig. 12, two branches with positive and negative heating-cooling ratios are observed. The exergy efficiency of demand scenarios in both branches correlate positively with the District DOC. Demand scenario CDF, which has the largest District DOC, also has the largest exergy efficiency (36.8 %). Demand scenarios with a positive heating-cooling ratio show a larger exergy efficiency. This results from the fact that in the calculation of the exergy efficiency, benefits from covered heating demands (heat flow at 60 °C) are weighted more heavily than covered cooling demands (heat flow close to ambient temperature). The coloring in Fig. 13 indicates the specific supply costs. It is remarkable that exergy efficiency only correlates with supply costs for demand scenarios with $R > 0$. However, a general correlation between exergy efficiency and supply costs cannot be observed.

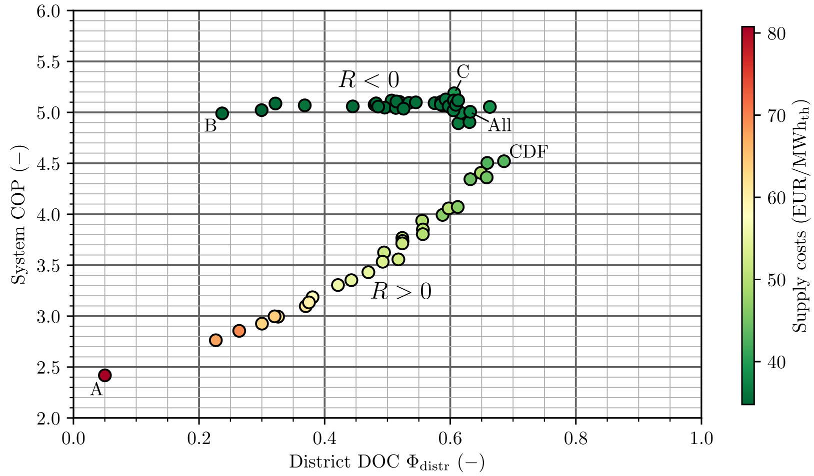

Figure 14: System coefficient of performance plotted against District DOC: For scenarios with more heating demands than cooling demands, the System COP increases with larger District DOCs. A correlation between System COP and supply costs is observed.

In Fig. 14, the System COP is plotted against the District DOC. In contrast to the exergy efficiency, a strong correlation between System COP and supply costs can be observed. This is due to the fact that, in terms of benefit, heating and cooling demands are weighted equally in the System COP (Eq. (24)) as well as in the specific supply costs (Eq. (20)).

4.3.1. Comparison with reference system

In this section, the performance of a district energy system with BLTN is compared with the performance of the reference system (c.f. Section 2.2.3) for all 63 demand scenarios. Intervals of the District DOC are identified for which the BLTN system performs better than the reference system.

In Fig. 15, the specific supply costs and the District DOC are depicted for the BLTN system and the reference system. The two branches ($R >$

0 and $R < 0$) are identified for the reference system as well. For $R > 0$ (heating demand larger than cooling demand), the supply costs of the reference system decrease with increasing District DOC. This results from the fact that cooling demands can be covered at lower costs compared to heating demands: The COP of chillers always exceeds 5, whereas the COP of air source heat pumps ranges between 2.9 and 4.5 (depending on the ambient air temperature). Therefore, the supply costs decrease for an increasing share of cooling demands. The overall trend for both systems (BLTN and reference system) is the same. However, the offset and slope of the trend lines are different. For demand scenarios with a small District DOC ($\Phi_{\mathrm{distr}} < 0.4$), the supply costs of the BLTN system are higher than the reference system. On the other hand, for large District DOCs ($\Phi_{\mathrm{distr}} > 0.45$), the BLTN system has lower supply costs than the reference system. This results from cost savings in the BLTN system with increasing demand balancing potential. A high District DOC indicates that a large proportion of heating demands can be supplied by waste heat from cooling applications. As a result, the overall efficiency increases and the supply costs decrease. In the reference system, a large overlap of heating and cooling demands does not lead to a higher overall efficiency since heating and cooling demands are covered separately from each other. As a result, BLTN systems become more efficient with larger District DOCs.

This effect is also reflected by the exergy efficiencies. Fig. 16 shows the exergy efficiency of all demand scenarios. For the BLTN system, the demand scenario with the largest District DOC has the highest exergy efficiency. The exergy efficiency of the reference system ranges between 24 % and 31 %, and

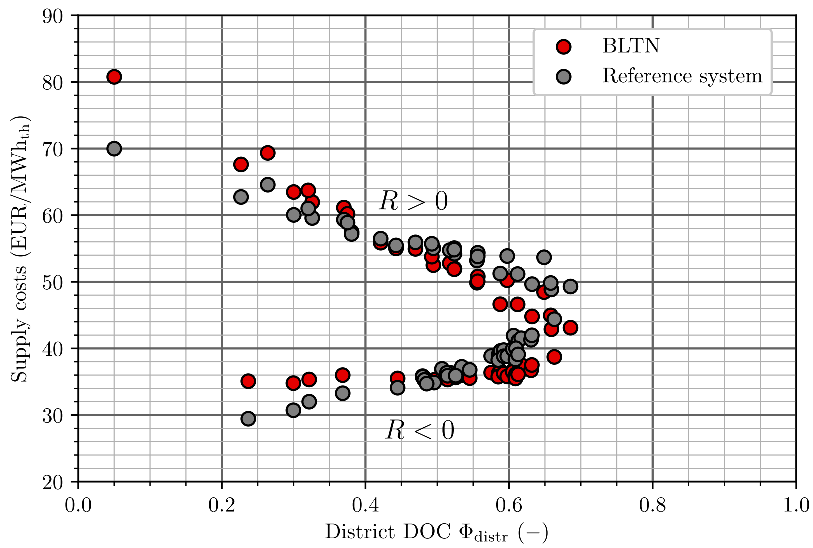

Figure 15: Supply costs and District DOC of the BLTN system and the reference system. For large District DOCs ($\Phi_{distr} > 0.45$), the system with BLTN has lower specific supply costs than the reference system.

thus varies less with different District DOCs. The reference system has a larger exergy efficiency than the BLTN system for District DOCs smaller than 0.25. For District DOCs larger than 0.3, the exergy efficiency of the BLTN system is higher than the reference system. This is in line with the findings by Pass et al. [34], who show that for the special case of a (static) demand situation with at least 1 unit cooling per 5.7 units of heating demand, a BLTN is more exergy efficient than a supply with decentral building energy systems (heat pumps and direct cooling). A (static) demand ratio of 1:5.7 equals a DOC of 0.298 and therefore affirms our findings (DOC = 0.3). The substantial increase of the exergy efficiency of the BLTN system with larger District DOCs is a result of the increased demand balancing potential. For large District DOCs, a large proportion of waste heat from chillers can be used as heat source for heat pumps and less thermal energy must be provided by the energy hub.

5. Conclusions

The efficiency and profitability of district energy systems with BLTN strongly depend on the heating and cooling demand structure of the connected buildings. BLTNs are best suited when heating and cooling demands are of the same magnitude and occur simultaneously. In this paper, the DOC is introduced which quantifies the simultaneity of heating and cooling demands. The DOC can be calculated for a district (District DOC), a building energy system (BES DOC) and a thermal network (Network DOC). Based on the use case, 63 demand scenarios are generated in order to investigate correlations between DOCs and key performance indicators.

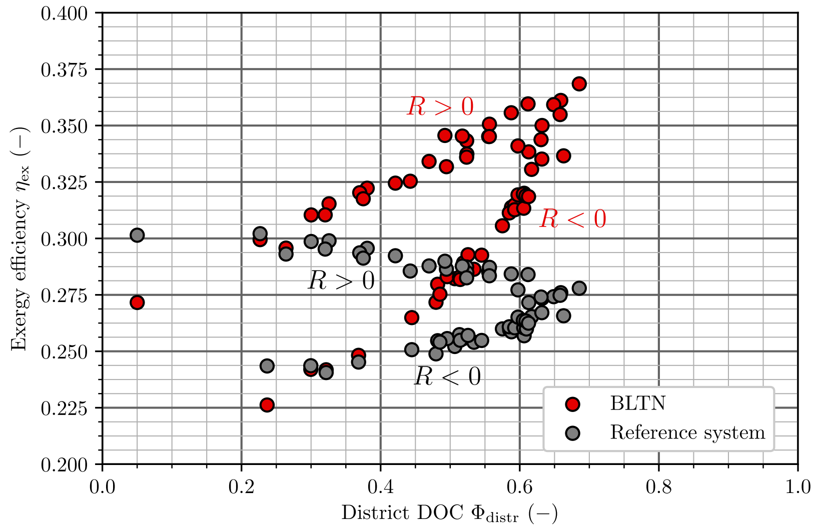

Figure 16: Exergy efficiency and District DOC of the system with BLTN and the reference system. For demand scenarios with a District DOC larger than 0.3, the exergy efficiency of the system with BLTN is higher than in the reference system.

A distinctive correlation between the Network DOC, mean BES DOC and District DOC is observed, from which the approximation $(1-\Phi_{\text{netw}})(1-\overline{\Phi}_{\text{BES}}) \approx (1-\Phi_{\text{distr}})$ is derived. This means, the District DOC alone is sufficient to estimate which proportion of demands can be balanced in buildings and the BLTN. This is an important finding since for the calculation of the District DOC no detailed knowledge about the network or building energy systems is needed. The District DOC is calculated solely with the buildings' heating and cooling demands which usually are available in an early planning phase of district energy systems. This makes the District DOC a widely applicable key metric in the planning process.

The analysis of the demand scenarios shows that the District DOC correlates with the system's exergy efficiency: The demand scenario with the largest District DOC has the highest exergy efficiency. For District DOCs larger than 0.3, a heating and cooling supply with a BLTN has a higher exergy efficiency compared to a reference system. This is in line with the findings by Pass et al. [34]. Moreover, district energy systems with BLTN have lower specific supply costs than a state-of-the-art reference system if the District DOC exceeds 0.45. The better economic and thermodynamic performance of systems with large District DOC is a result of the larger potential for balancing demands in the districts.

In summary, this study shows the importance of the district's demand structure for planning district energy systems and BLTN systems in particular. The District DOC turns out to be a meaningful metric which allows to characterize the demand structure of a district. Thus, the District DOC helps to identify clusters of buildings with complementary heating and cooling demand profiles and to decide which buildings should be connected to a BLTN.

In future works, the DOC metric can be extended in order to consider balancing effects that are achieved by central thermal storages in a BLTN. Calculating a DOC for a central storage can help to quantify to what extend the demand balancing can be increased by installing the storage, and to determine an optimal storage capacity as it is a trade-off between investment and demand balancing potential. In addition, heat losses of the network can be included in the DOC calculation as they also contribute to the balancing of heating and cooling demands.

6. Acknowledgments

This work was supported by the Helmholtz Association under the Joint Initiative "Energy System 2050 – A Contribution of the Research Field Energy".

7. Nomenclature

Abbreviations

5GDHC	5th generation district heating and cooling
ASHP	Air source heat pump
BAT	Battery
BES	Building energy system
BLTN	Bidirectional low temperature network
CC	Compression chiller
DOC	Demand overlap coefficient
EH	Energy hub
HP	Heat pump
ISHP	Ice storage heat pump
ITES	Ice thermal energy storage
KPI	Key performance indicator
O&M	Operation and maintenance
TAC	Total annualized costs
TES	Thermal energy storage
PV	Photovoltaics

Indices and Sets

$b \in \mathrm{B}$	Buildings
$t \in \mathrm{T}$	Time steps

Variables

c	Specific supply costs
COP_{Sys}	System COP
e	CO_2 emissions
P	Electric power
Q	Thermal energy
$\dot{Q}$	Thermal power
T	Temperature
W	Electric energy
Φ	Demand Overlap Coefficient

Parameters

kA	Heat loss coefficient
R	Demand ratio
COP	Coefficient of performance
η	Efficiency

Subscripts

bal	balancing
c	cooling
dem	demand
distr	district
h	heating
netw	network
ref	reference
res	residual
ret	return
sup	supply
th	thermal
tot	total

Appendix A. Building data

Detailed data about the 17 buildings is provided in Table A.4.

Appendix B. Linear program

The linear program is based on an optimization model by Wirtz et al. [35]. In this section, all model differences compared to the formulation in [35] are presented in detail. All model parameters which are not presented in [35] or have been modified are listed in Appendix B.4.

Appendix B.1. Objective function

The objective function are total annualized costs (TAC), which are based on VDI 2067 [40] and include annualized investments of the equipment of the energy hub (C_{EH}) and the building energy systems (C_{BES}), electricity costs (C_{el}) and revenues from electricity feed-in ($R_{\mathrm{feed-in}}$) as well as investment for the thermal network (C_{netw}):

$$TAC = C_{\mathrm{EH}} + C_{\mathrm{BES}} + C_{\mathrm{el}} - R_{\mathrm{feed-in}} + C_{\mathrm{netw}} \tag{B.1}$$

The definitions of the cost proportions do not differ from the ones presented in [35].

Appendix B.2. Building energy system (BES)

The constraints of the building energy system remain unchanged except for the following adaptions: Firstly, it is assumed that the heat storage is ideally stratified. The heat pump (with a supply temperature of 60 °C) can charge the storage regardless of its state of charge and heat from the heat storage can always be used to cover the buildings heat demand (at 60 °C). Therefore the following constraint from the original formulation is omitted without substitution:

$$\dot{Q}_{\mathrm{h,EB},b,d,t} \geq \dot{Q}^{\mathrm{ch}}_{\mathrm{h,TES},b,d,t} \quad \forall \;\; b \in \mathrm{B}, \;\; d \in \mathrm{D}, \;\; t \in \mathrm{T} \tag{B.2}$$

$\dot{Q}_{\mathrm{h,EB},b,d,t}$ denotes the heat output of the electric boiler (EB) and $\dot{Q}^{\mathrm{ch}}_{\mathrm{h,TES},b,d,t}$ the heat flow charging the heat storage. The storage is assumed to be charged and discharged directly without additional heat exchangers. Therefore, all losses related to the charging and discharging process are neglected ($\eta^{\mathrm{ch}}_{\mathrm{TES}} = \eta^{\mathrm{dch}}_{\mathrm{TES}} = 1$).

Furthermore, some constraints are simplified due to the absence of cooling towers in the building energy systems. In particular, the cooling balance of a building is reduced to

$$\dot{Q}_{\mathrm{c,CC},b,d,t} + \dot{Q}_{\mathrm{c,DRC},b,d,t} = \dot{Q}_{\mathrm{c,dem},b,d,t} \quad \forall \;\; b \in \mathrm{B}, \;\; d \in \mathrm{D}, \;\; t \in \mathrm{T} \qquad \text{(B.3)}$$

Here, $\dot{Q}_{\mathrm{c,CC},b,d,t}$ denotes the cooling power of the compression chiller (CC) and $\dot{Q}_{\mathrm{c,DRC},b,d,t}$ the cooling power of the direct cooler (DRC).

Appendix B.3. Energy hub (EH)

The superstructure of the energy hub is changed substantially compared to the formulation in [35]. Therefore, all constraints for the energy hub are explained in detail.

Generation units and storages

The thermal or electric power of the units is limited by their rated power:

$$\dot{Q}_{\mathrm{h},k,\mathrm{EH},d,t} \leq \dot{Q}^{\mathrm{nom}}_{\mathrm{h},k,\mathrm{EH}} \quad \forall \; k \in \{\mathrm{ASHP}, \mathrm{ISHP}\}, \; d \in \mathrm{D}, \; t \in \mathrm{T} \qquad \text{(B.4)}$$

$$\dot{Q}_{\mathrm{c,ASHP,EH},d,t} \leq \dot{Q}^{\mathrm{nom}}_{\mathrm{c,ASHP,EH}} \quad \forall \; d \in \mathrm{D}, \; t \in \mathrm{T} \qquad \text{(B.5)}$$

$$P_{\mathrm{PV,EH},d,t} \leq P^{\mathrm{nom}}_{\mathrm{PV,EH}} \quad \forall \; d \in \mathrm{D}, \; t \in \mathrm{T} \qquad \text{(B.6)}$$

The capacity of the reversible air source heat pump $cap_{\mathrm{ASHP,EH}}$ which is needed to calculate the investment is defined by the constraints

$$\dot{Q}^{\mathrm{nom}}_{\mathrm{h,ASHP,EH}} \leq cap_{\mathrm{ASHP,EH}} \qquad \text{(B.7)}$$

$$\dot{Q}^{\mathrm{nom}}_{\mathrm{c,ASHP,EH}} \leq cap_{\mathrm{ASHP,EH}} \qquad \text{(B.8)}$$

The total module area of PV (A_{PV}) is limited by the maximum available area:

$$A_{\mathrm{PV}} \leq A^{\mathrm{max}}_{\mathrm{PV}} \qquad \text{(B.9)}$$

The rated power of the PV modules is

$$P^{\mathrm{nom}}_{\mathrm{PV,EH}} = G_{\mathrm{sol,STC}} A_{\mathrm{PV}} \, \eta_{\mathrm{PV,STC}} \qquad \text{(B.10)}$$

Here, $G_{\mathrm{sol,STC}}$ denotes the global tilted irradiance and $\eta_{\mathrm{PV,STC}}$ the electric efficiency under Standard Test Conditions. The power of the PV modules is

$$P_{\mathrm{PV,EH},d,t} \leq G_{\mathrm{sol},d,t} A_{\mathrm{PV}}\, \eta_{\mathrm{PV},d,t} \quad \forall \;\; d \in \mathrm{D}, \;\; t \in \mathrm{T} \tag{B.11}$$

For energy conversion units constant or time-dependent efficiencies are assumed. For the air source heat pump (ASHP), a heating and cooling COP ($COP_{\mathrm{h,ASHP},d,t}$ / $COP_{\mathrm{c,ASHP},d,t}$) is calculated a priori with the ambient air temperature. The input-output constraints are

$$\dot{Q}_{\mathrm{h,ASHP,EH},d,t} = P_{\mathrm{h,ASHP,EH},d,t}\, COP_{\mathrm{h,ASHP},d,t} \quad \forall \;\; d \in \mathrm{D}, \;\; t \in \mathrm{T} \tag{B.12}$$

$$\dot{Q}_{\mathrm{c,ASHP,EH},d,t} = P_{\mathrm{c,ASHP,EH},d,t}\, COP_{\mathrm{c,ASHP},d,t} \quad \forall \;\; d \in \mathrm{D}, \;\; t \in \mathrm{T} \tag{B.13}$$

$$P_{\mathrm{ASHP,EH},d,t} = P_{\mathrm{h,ASHP,EH},d,t} + P_{\mathrm{c,ASHP,EH},d,t} \quad \forall \;\; d \in \mathrm{D}, \;\; t \in \mathrm{T} \tag{B.14}$$

$P_{\mathrm{ASHP,EH},d,t}$ denotes the total power demand of the air source heat pump. For discharging the ice thermal energy storage (ITES), an ice storage heat pump (ISHP) has to be installed, which freezes the fluid in the storage. The efficiency of the ISHP ($COP_{\mathrm{h,ISHP},d,t}$) is calculated a priori based on the storage temperature (assumed 0 °C) and the temperature of the warm pipe of the BLTN:

$$\dot{Q}_{\mathrm{h,ISHP,EH},d,t} = P_{\mathrm{ISHP,EH},d,t}\, COP_{\mathrm{h,ISHP},d,t} \quad \forall \;\; d \in \mathrm{D}, \;\; t \in \mathrm{T} \tag{B.15}$$

$$\dot{Q}_{\mathrm{h,ISHP,EH},d,t} = \dot{Q}^{\mathrm{dch}}_{\mathrm{h,ITES,EH},d,t} + P_{\mathrm{ISHP,EH},d,t} \quad \forall \;\; d \in \mathrm{D}, \;\; t \in \mathrm{T} \tag{B.16}$$

The ice storage is charged by passing water from the warm pipe of the BLTN through the pipes of the ice storage (no auxiliary power needed).

Storages are modeled with a formulation that allows a seasonal operation (as presented by [41] and [42]) and in accordance with the formulation in

[35]. The ice thermal energy storage is modeled in the same manner except for minor changes: The standby losses of the ice storage do not depend on its state of charge since the temperature is assumed constant (0 °C). Therefore, losses only depend on the storage capacity (i.e. storage surface area):

$$S^{\mathrm{cap}}_{\mathrm{ITES,EH}} \phi_{\mathrm{ITES,EH,loss}} \tag{B.17}$$

Furthermore, the charging power is limited by a fixed value instead of a capacity share:

$$\dot{Q}^{\mathrm{ch}}_{\mathrm{c,ITES,EH},d,t} \leq \dot{Q}^{\mathrm{ch,max}}_{\mathrm{c,ITES,EH}} \quad \forall \;\; d \in \mathrm{D}, \quad t \in \mathrm{T} \tag{B.18}$$

The discharging power of the ITES is constrained by the operation limits of the ice storage heat pump according to Eq. (B.16).

Energy balances

The thermal balance of the energy hub is:

$$\begin{aligned} &\dot{Q}_{\mathrm{h,ASHP,EH},d,t} + \dot{Q}_{\mathrm{h,ISHP,EH},d,t} - \dot{Q}_{\mathrm{c,ASHP,EH},d,t} \\ &- \dot{Q}^{\mathrm{ch}}_{\mathrm{c,ITES,EH},d,t} = \dot{Q}_{\mathrm{res,EH},d,t} + \dot{Q}_{\mathrm{netw},d,t} \\ &\forall \;\; d \in \mathrm{D}, \quad t \in \mathrm{T} \end{aligned} \tag{B.19}$$

Here, $\dot{Q}_{\mathrm{h,ASHP,EH},d,t}$ and $\dot{Q}_{\mathrm{h,ISHP,EH},d,t}$ describe the heat from the ASHP and ISHP, respectively. $Q_{\mathrm{c,ASHP,EH},d,t}$ denotes the cooling power of the ASHP and $\dot{Q}^{\mathrm{ch}}_{\mathrm{c,ITES,EH},d,t}$ denotes the thermal charging power of the ice storage. $\dot{Q}_{\mathrm{res,EH},d,t}$ and $\dot{Q}_{\mathrm{netw},d,t}$ denote the residual heat demand of all buildings (including thermal network losses) and the heat needed to raise or lower the temperature of the BLTN, respectively. The electricity balance of the energy hub is

$$P_{\text{PV,EH},d,t} + P_{\text{grid},d,t} + P^{\text{dch}}_{\text{BAT,EH},d,t} = \sum_{b \in B} P_{\text{BES},b,d,t} + P_{\text{pumps},d,t}$$
$$+ P_{\text{ASHP,EH},d,t} + P_{\text{ISHP,EH},d,t} + P_{\text{feed-in},d,t} + P^{\text{ch}}_{\text{BAT,EH},d,t}$$
$$\forall \;\; d \in \text{D}, \quad t \in \text{T} \tag{B.20}$$

Here, $\sum_{b \in B} P_{\text{BES},b,d,t}$ denotes the cumulated power demand by heat pumps, compression chillers and electric boilers in the buildings. $P_{\text{grid},d,t}/P_{\text{feed-in},d,t}$ denote the electric energy taken from and fed into the public power grid, respectively. The electric demands of the hydraulic pumps $P_{\text{pumps},d,t}$ are calculated a priori as described in [35].

Appendix B.4. Model parameters

In this section, all model parameters which are not presented in [35] or have been modified compared to the original formulation are listed. The heat pump COPs (ASHP and ISHP) are calculated with the Carnot efficiency:

$$COP_{\text{h}} = \eta_{\text{Carnot}} COP_{\text{Carnot}} = \eta_{\text{Carnot}} \frac{T_{\text{sink}}}{T_{\text{sink}} - T_{\text{source}}} \tag{B.21}$$

Similarly, for the cooling mode of the ASHP

$$COP_{\text{c}} = \eta_{\text{Carnot}} \frac{T_{\text{source}}}{T_{\text{sink}} - T_{\text{source}}} \tag{B.22}$$

is applied. In Eq. (B.21) and (B.22), T_{sink} and T_{source} denote the condensing temperature and evaporating temperature of the refrigerant, respectively. For each heat transfer, a minimal temperature difference ΔT^{min} between the two sides of the heat exchanger is considered. $\Delta T^{\text{min}} = 2\,\text{K}$ is applied in case of water to water heat transfer and $\Delta T^{\text{min}} = 10\,\text{K}$ in case of water to air.

Table B.5 shows the Carnot efficiencies η_{Carnot} used for the COP calculation. As described in [35], COP_{h} is limited by 7 and COP_{c} by 6.

All technical parameters of the ice storage are listed in Table B.6. Economic parameters are shown in Table B.7.

For the use case presented in Section 3.1, the annualized costs of the thermal network are $C_{\mathrm{netw}} = 28.3\,\mathrm{kEUR/a}$. The total heat transmittance of the network is $(kA)_{\mathrm{tot}} = 3.66\,\mathrm{kW/K}$. Hydraulic pumps with a total electric capacity of 9.32 kW and a total annual electricity demand of 10.44 MWh are installed. As explained in Section 4.1, 63 demand scenarios are generated by defining subsets of buildings clusters. In the original model formulation, annualized costs for the network infrastructure (pipe costs and earthworks) as well as pumping work are considered, which both are calculated prior to the optimization. For evaluating the demand scenarios, a network topology is not designed for each demand scenario a priori. Instead, the pump work, network costs and the heat loss coefficient of the network (kA_{tot}), which were calculated for the use case with 17 buildings, are scaled linearly with the total heating and cooling demands of the respective demand scenario. The resulting error is small since the pump work, heat losses and network costs are small compared to the other energy flows and cost proportions [35]. For the CO_2 emission calculation, a CO_2 factor of 516 g/kWh is assumed for imported power from the electricity grid.

Appendix C. Optimal energy system design

The optimal energy system design for the use case in Section 3 is listed in Table C.8 (energy hub) and Table C.9 (building energy systems). The

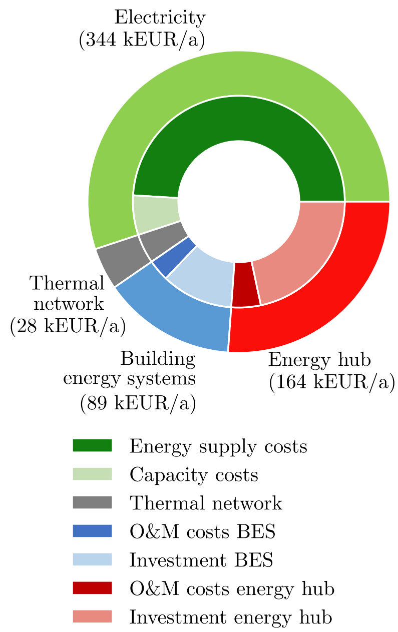

Figure C.17: Proportions of total annualized costs.

proportions of the total annualized costs are depicted in Fig. C.17.

Table A.4: Building data and demands.

Buildings	$\dot{Q}^{\text{tot}}_{\text{h,dem}}$ [MWh]	$\dot{Q}^{\text{tot}}_{\text{c,dem}}$ [MWh]	Function —	R —	Net floor area m^2
1	1352	490	Office/Lab	0.47	3166
2	1209	84	Canteen	0.87	4118
3	302	3426	Data center	-0.84	4235
4	685	3920	Data center	-0.70	6923
5	455	119	Laboratory	0.59	954
6	640	220	Office/Lab	0.49	2559
7	138	38	Office/Lab	0.57	665
8	91	15	Laboratory	0.72	1106
9	497	1063	Office/Lab	-0.36	7996
10	33	71	Office	-0.37	888
11	35	129	Office	-0.58	2968
12	350	168	Laboratory	0.35	1188
13	239	0	Office/Lab	1	4854
14	107	109	Laboratory	-0.01	240
15	5	131	Laboratory	-0.93	401
16	21	59	Office	-0.47	1210
17	201	0	Office	1	1371

Table B.5: Carnot efficiencies for COP calculation.

	ASHP	ISHP
η_{Carnot} [$-$]	0.4	0.5

Table B.6: Technical parameters of the ice thermal energy storage.

$\eta^{\mathrm{ch}}\,[-]$	$\eta^{\mathrm{dch}}\,[-]$	$\dot{Q}^{\mathrm{ch,max}}\,[\mathrm{MW}]$	$\phi_{\mathrm{loss}}\,[-]$
0.95	0.95	0.3	0.001

$T\,[^{\circ}\mathrm{C}]$	$s^{\mathrm{min}}\,[-]$	$s^{\mathrm{max}}\,[-]$	$S^{\mathrm{cap,max}}\,[\mathrm{MW}]$
0	0	1	10

Table B.7: Economic parameters.

	ASHP	ITES	ISHP
Specific investment i $\left[\frac{\mathrm{kEUR}}{\mathrm{MW}}\right]$	350	15	250
Service life t_{L} [a]	20	20	20
Capital rec. factor a_{inv} [%]	8.02	8.02	8.02
Share for o&m f_{om} [%]	2.5	2	2.5

Table C.8: Installed capacity and operation of components in energy hub.

Technology	Capacity	Generation	Full load hours $\left[\frac{\mathrm{h}}{\mathrm{a}}\right]$
Air source heat pump	$1.95\,\mathrm{MW_{th}}$	$6042\,\mathrm{MWh_{th}}$	3099
Ice thermal energy storage	4.95 MWh	—	—
Ice storage heat pump	$0.04\,\mathrm{MW_{th}}$	$60\,\mathrm{MWh_{th}}$	1506
Photovoltaics	$1.02\,\mathrm{MW_{peak}}$	$1122\,\mathrm{MWh_{el}}$	1100
Battery	—	—	—

Table C.9: Installed capacity and operation of components in building energy systems.

Technology	Capacity	Generation	Full load hours $\left[\frac{h}{a}\right]$
Heat pump	$1.63\,MW_{th}$	$6400\,MWh_{th}$	3926
Electric boiler	$0.78\,MW_{th}$	$12\,MWh_{th}$	15
Comp. chiller	—	—	—
Direct cooling	$2.88\,MW_{th}$	$10042\,MWh_{th}$	3487
Thermal energy storage	2.44 MWh	—	—

References

[1] H. Lund, N. Duic, P. A. Østergaard, B. V. Mathiesen, Future district heating systems and technologies: On the role of smart energy systems and 4th generation district heating, Energy 165 (2018) 614–619 (2018). doi:10.1016/j.energy.2018.09.115.

[2] P. Simeoni, G. Ciotti, M. Cottes, A. Meneghetti, Integrating industrial waste heat recovery into sustainable smart energy systems, Energy 175 (2019) 941–951 (2019). doi:10.1016/j.energy.2019.03.104.

[3] G. R. Truedsson, Industrial waste heat recovery - a case in point, Energy Engineering: Journal of the Association of Energy Engineering 97 (1) (2000) 23–28, 31 (2000).

[4] O.M. Al-Rabghi, M. Beirutty, M. Akyurt, Y. Najjar, T. Alp, Recovery and utilization of waste heat, Heat Recovery Systems and CHP 13 (5) (1993) 463–470 (1993). doi:10.1016/0890-4332(93)90047-Y.

[5] H. Fang, J. Xia, K. Zhu, Y. Su, Y. Jiang, Industrial waste heat utilization for low temperature district heating, Energy Policy 62 (2013) 236–246 (2013). doi:10.1016/j.enpol.2013.06.104.

[6] A. Capozzoli, G. Primiceri, Cooling systems in data centers: State of art and emerging technologies, Energy Procedia 83 (2015) 484–493 (2015). doi:10.1016/j.egypro.2015.12.168.

[7] E. Oró, P. Taddeo, J. Salom, Waste heat recovery from urban air cooled data centres to increase energy efficiency of district heating

networks, Sustainable Cities and Society 45 (2019) 522–542 (2019). doi:10.1016/j.scs.2018.12.012.

[8] S. Petrović, A. Colangelo, O. Balyk, C. Delmastro, M. Gargiulo, M. B. Simonsen, K. Karlsson, The role of data centres in the future danish energy system, Energy (2020) 116928 (2020). doi:10.1016/j.energy.2020.116928.

[9] P. Huang, B. Copertaro, X. Zhang, J. Shen, I. Löfgren, M. Rönnelid, J. Fahlen, D. Andersson, M. Svanfeldt, A review of data centers as prosumers in district energy systems: Renewable energy integration and waste heat reuse for district heating, Applied Energy 258 (2020) 114109 (2020). doi:10.1016/j.apenergy.2019.114109.

[10] L. Brange, J. Englund, P. Lauenburg, Prosumers in district heating networks – a swedish case study, Applied Energy 164 (2016) 492–500 (2016). doi:10.1016/j.apenergy.2015.12.020.

[11] B. Sanner, R. Kalf, A. Land, K. Mutka, P. Papillon, G. Stryi-Hipp, W. Weiss, 2020-2030-2050, Common vision for the renewable heating and cooling sector in Europe: European technology platform on renewable heating and cooling, Publications Office, Luxembourg, 2011 (2011).

[12] U. Persson, M. Münster, Current and future prospects for heat recovery from waste in european district heating systems: A literature and data review, Energy 110 (2016) 116–128 (2016). doi:10.1016/j.energy.2015.12.074.

[13] Borna Doračić, Tomislav Novosel, Tomislav Pukšec and Neven Duić, Evaluation of excess heat utilization in district heating systems by implementing levelized cost of excess heat, Energies 11 (3) (2018) 575 (2018). doi:10.3390/en11030575.

[14] A. Kapil, I. Bulatov, R. Smith, J.-K. Kim, Process integration of low grade heat in process industry with district heating networks, Energy 44 (1) (2012) 11–19 (2012). doi:10.1016/j.energy.2011.12.015.

[15] H. Jouhara, N. Khordehgah, S. Almahmoud, B. Delpech, A. Chauhan, S. A. Tassou, Waste heat recovery technologies and applications, Thermal Science and Engineering Progress 6 (2018) 268–289 (2018). doi:10.1016/j.tsep.2018.04.017.

[16] F. Bünning, M. Wetter, M. Fuchs, D. Müller, Bidirectional low temperature district energy systems with agent-based control: Performance comparison and operation optimization, Applied Energy 209 (2018) 502–515 (2018). doi:10.1016/j.apenergy.2017.10.072.

[17] A. Prasanna, V. Dorer, N. Vetterli, Optimisation of a district energy system with a low temperature network, Energy 137 (2017) 632–648 (2017). doi:10.1016/j.energy.2017.03.137.

[18] S. Buffa, M. Cozzini, M. D'Antoni, M. Baratieri, R. Fedrizzi, 5th generation district heating and cooling systems: A review of existing cases in europe, Renewable and Sustainable Energy Reviews 104 (2019) 504–522 (2019). doi:10.1016/j.rser.2018.12.059.

[19] The European Comission, Fifth generation, low temperature, high exergy district heating and cooling networks.
URL `https://cordis.europa.eu/project/rcn/194622/factsheet/en`

[20] S. Boesten, W. Ivens, S. C. Dekker, H. Eijdems, 5th generation district heating and cooling systems as a solution for renewable urban thermal energy supply, Advances in Geosciences 49 (2019) 129–136 (2019). doi:10.5194/adgeo-49-129-2019.

[21] J. von Rhein, G. P. Henze, N. Long, Y. Fu, Development of a topology analysis tool for fifth-generation district heating and cooling networks, Energy Conversion and Management 196 (2019) 705–716 (2019). doi:10.1016/j.enconman.2019.05.066.

[22] M. Pellegrini, A. Bianchini, The innovative concept of cold district heating networks: A literature review, Energies 11 (1) (2018) 236 (2018). doi:10.3390/en11010236.

[23] F. Ruesch, M. Haller, Potential and limitations of using low-temperature district heating and cooling networks for direct cooling of buildings, Energy Procedia 122 (2017) 1099–1104 (2017). doi:10.1016/j.egypro.2017.07.443.

[24] T. Sommer, S. Mennel, M. Sulzer, Lowering the pressure in district heating and cooling networks by alternating the connection of the expansion vessel, Energy 172 (2019) 991–996 (2019). doi:10.1016/j.energy.2019.02.010.

[25] W. H. Song, Y. Wang, A. Gillich, A. Ford, M. Hewitt, Modelling development and analysis on the balanced energy networks (ben) in london, Applied Energy 233-234 (2019) 114–125 (2019). doi:10.1016/j.apenergy.2018.10.054.

[26] T. Blacha, M. Mans, P. Remmen, D. Müller, Dynamic simulation of bidirectional low-temperature networks - a case study to facilitate the integration of renewable energies, Building Simulation Conference, Rome, Italy (2019).

[27] R. Rogers, V. Lakhian, M. Lightstone, J. S. Cotton, Modeling of low temperature thermal networks using historical building data from district energy systems, in: Proceedings of the 13th International Modelica Conference, Regensburg, Germany, March 4–6, 2019, Linköping Electronic Conference Proceedings, Linköping University Electronic Press, 2019, pp. 543–550 (2019). doi:10.3384/ecp19157543.

[28] H. Lund, S. Werner, R. Wiltshire, S. Svendsen, J. E. Thorsen, F. Hvelplund, B. V. Mathiesen, 4th generation district heating (4gdh) integrating smart thermal grids into future sustainable energy systems, Energy 68 (2014) 1–11 (2014). doi:10.1016/j.energy.2014.02.089.

[29] M. Wahlroos, M. Pärssinen, S. Rinne, S. Syri, J. Manner, Future views on waste heat utilization – case of data centers in northern europe, Renewable and Sustainable Energy Reviews 82 (2018) 1749–1764 (2018). doi:10.1016/j.rser.2017.10.058.

[30] M. Wahlroos, M. Pärssinen, J. Manner, S. Syri, Utilizing data cen-

ter waste heat in district heating – impacts on energy efficiency and prospects for low-temperature district heating networks, Energy 140 (2017) 1228–1238 (2017). doi:10.1016/j.energy.2017.08.078.

[31] M. Papapetrou, G. Kosmadakis, A. Cipollina, U. La Commare, G. Micale, Industrial waste heat: Estimation of the technically available resource in the eu per industrial sector, temperature level and country, Applied Thermal Engineering 138 (2018) 207–216 (2018). doi:10.1016/j.applthermaleng.2018.04.043.

[32] U. Persson, S. Werner, District heating in sequential energy supply, Applied Energy 95 (2012) 123–131 (2012). doi:10.1016/j.apenergy.2012.02.021.

[33] E. Woolley, Y. Luo, A. Simeone, Industrial waste heat recovery - a systematic approach, Sustainable Energy Technologies and Assessments 29 (2018) 50–59 (2018).

[34] R. Zarin Pass, M. Wetter, M. A. Piette, A thermodynamic analysis of a novel bidirectional district heating and cooling network, Energy 144 (2018) 20–30 (2018). doi:10.1016/j.energy.2017.11.122.

[35] M. Wirtz, L. Kivilip, P. Remmen, D. Müller, 5th generation district heating: A novel design approach based on mathematical optimization, Applied Energy 260 (2020). doi:10.1016/j.apenergy.2019.114158.

[36] A. Kallert, D. Schmidt, T. Bläse, Exergy-based analysis of renewable multi-generation units for small scale low temperature dis-

trict heating supply, Energy Procedia 116 (2017) 13–25 (2017). doi:10.1016/j.egypro.2017.05.051.

[37] Ş. Kılkış, C. Wang, F. Björk, I. Martinac, Cleaner energy scenarios for building clusters in campus areas based on the rational exergy management model, Journal of Cleaner Production 155 (2017) 72–82 (2017). doi:10.1016/j.jclepro.2016.10.126.

[38] S. Jansen, N. Woudstra, Understanding the exergy of cold: theory and practical examples, International Journal of Exergy 7 (6) (2010) 693 (2010). doi:10.1504/IJEX.2010.035516.

[39] M. A. Rosen, M. N. Le, I. Dincer, Efficiency analysis of a cogeneration and district energy system, Applied Thermal Engineering 25 (1) (2005) 147–159 (2005). doi:10.1016/j.applthermaleng.2004.05.008.

[40] VDI 2067-1. Economic efficiency of building installations - Fundamentals and economic calculation. Technical report., Beuth Verlag GmbH (2012).

[41] L. Kotzur, P. Markewitz, M. Robinius, D. Stolten, Time series aggregation for energy system design: Modeling seasonal storage, Applied Energy 213 (2018) 123–135 (2018). doi:10.1016/j.apenergy.2018.01.023.

[42] P. Gabrielli, M. Gazzani, E. Martelli, M. Mazzotti, A milp model for the design of multi-energy systems with long-term energy storage, in: 27th European Symposium on Computer Aided Process Engineering, Vol. 40 of Computer Aided Chemical Engineering, Elsevier, 2017, pp. 2437–2442 (2017). doi:10.1016/B978-0-444-63965-3.50408-6.